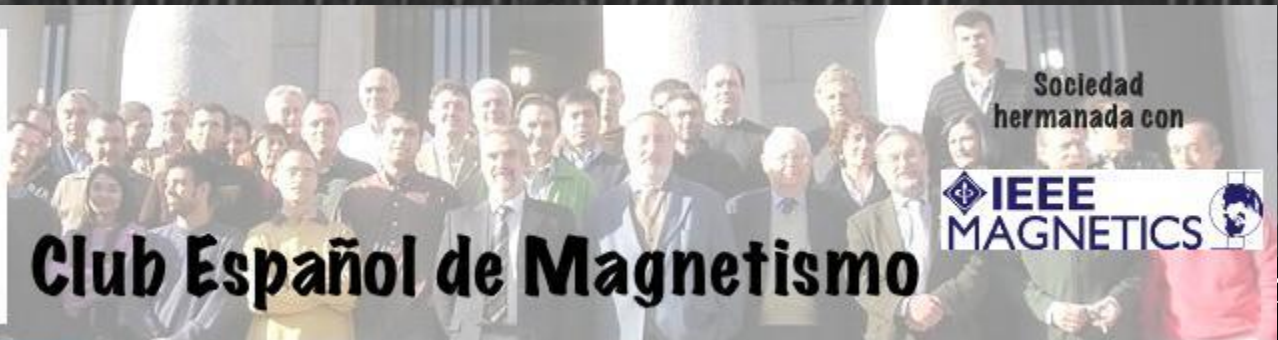
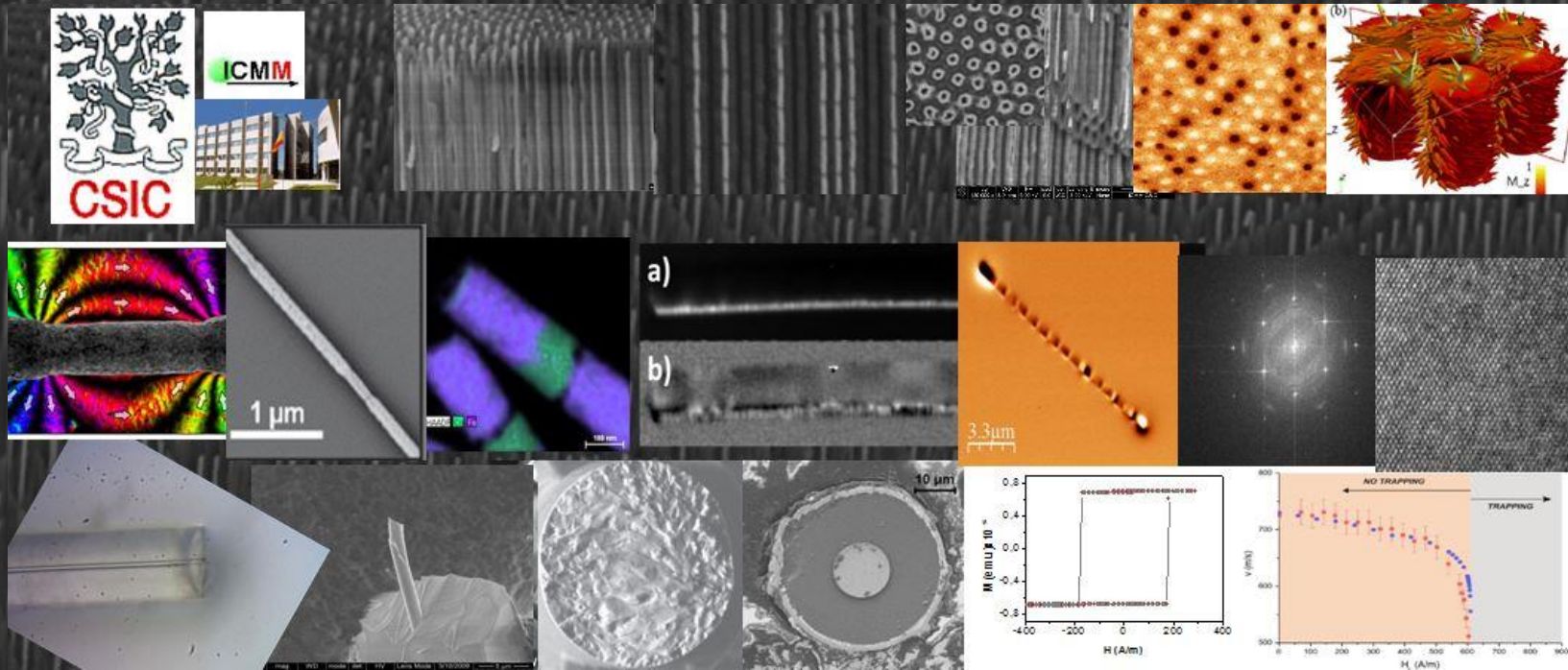


Nano y Microhilos Magnéticos

Manuel Vázquez Villalabeitia



Nano y Microhilos Magnéticos

- *Whiskers de hierro (tesina y tesis), (1974-80)*
- *Cintas Amorfas (postdocs), anisotropías magnetoelásticas (1981-91)*
- *Microhilos amorfos, GMI, Biestabilidad Magnética (1992-2000)*
- *Micro & Nanohilos, formación de un Laboratorio/Grupo (2001 - 2008)*
- *Nanohilos cilíndricos: estudios más recientes (2009-2017)*

- Laboratorio de Magnetismo UCM (5° Curso Físicas) 1974
Montaje de la práctica de Resonancia Magnética Nuclear

- Koninklijke/Shell laboratories, Amsterdam, Verano 1974
(Beca IAESTE)

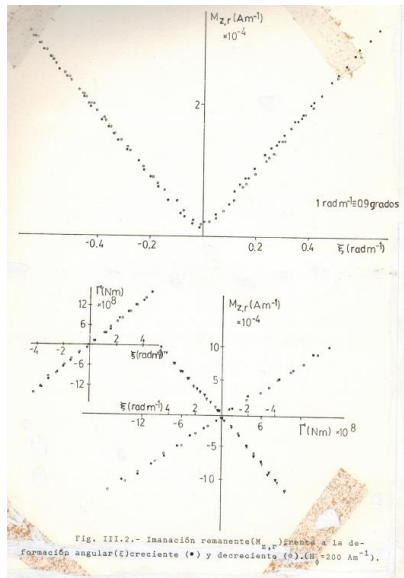
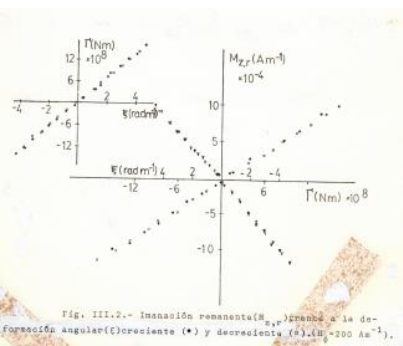
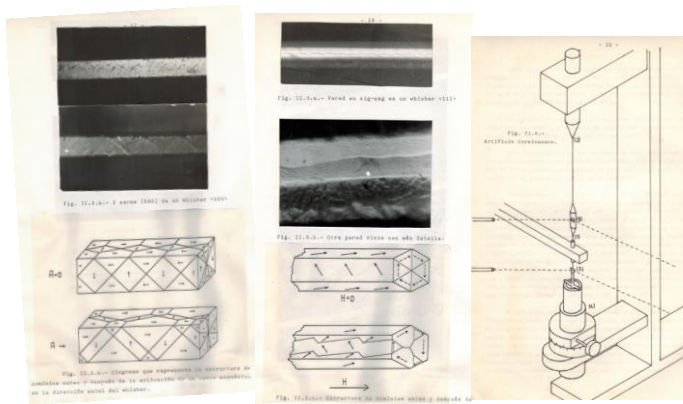
C^{13} Spin-Lattice relaxation times and Nuclear Overhauser effect of olefins adsorbed on Na exchanged zeolites

Tesina (Nov. 1974)



Tesis: Laboratorio de Magnetismo UCM, 1975-80

Efecto Wiedemann inverso in whiskers de hierro



Antonio Hernando, Director de Tesis



Louis Néel visita el grupo de Salvador Velayos, 1978

IEEE Transactions on Magnetics Vol. MAG-13, No. 5, September 1977

INVERSE WIEDEMANN EFFECT IN $\langle 100 \rangle$ IRON WHISKERS

A. Hernando, M. Vázquez, V. Madurga and J. Becerril

Lab. of Magnetism. University Complutense Madrid. Spain

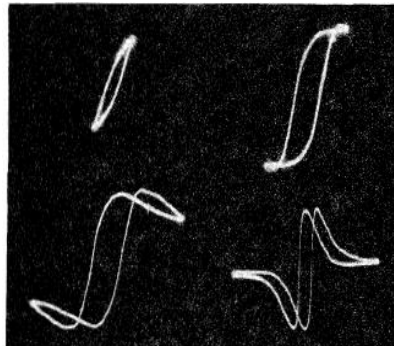


Figure 2. $M-H$ curves for the whisker u-1 twisted 5° . The amplitude of circular field is: 0.1, 0.3, 0.6 and 1 ($\times 1000$) A/m

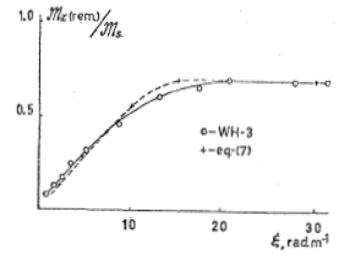


Figure 5. Experimental and theoretical curve for a $\langle 100 \rangle$ iron whisker

- Postdoc en Max-Planck-Institute für Metallforschung, Stuttgart, 1981-83 (Beca A.v. Humboldt)

Cintas amorfas: Anisotropía Magnetoelástica, Distribución de tensiones, Estructura de dominios, Aproximación a la saturación, Exponentes críticos

Max-Planck-Institut für Metallforschung, Institut für Physik, Stuttgart¹,
and Institut für Theoretische und Angewandte Physik der Universität Stuttgart

The Effect of Tensile Stresses on the Magnetic Properties of $\text{Co}_{55}\text{Fe}_5\text{Ni}_{10}\text{Si}_{11}\text{B}_{16}$ Amorphous Alloys

By
M. VÁZQUEZ², W. FERNENGEL, and H. KRONMÜLLER

Inserting (14), (6), and (19) into (30) we obtain

$$\chi^{-1} = -\frac{3\lambda_s}{\mu_0 M_s^2} \sigma \left\{ 1 - \frac{m_r(0) (\bar{\sigma}_c^2 / \sigma^2)}{1 - m_r(0) + (\bar{\sigma}_c / \sigma) [1 - 2m_r(0)]} \right\}$$

If we consider (27), (28), and

$$m_r(\infty) \approx \cos \varphi_{\perp} v_{\perp}^0 + \cos \varphi_{\parallel} v_{\parallel}^0,$$

where $m_r(\infty)$ is the value of m_r for very large applied stresses, we find

$$H_c = -\frac{3\lambda_s m_r(\infty)}{\mu_0 M_s} \frac{\sigma^2 + \sigma \bar{\sigma}_t + \sigma \sigma_c + \bar{\sigma}_t \sigma_c}{\sigma + (\bar{\sigma}_c v_{\perp}^0 + \bar{\sigma}_t v_{\parallel}^0)}.$$

Helmut Kronmüller supervisor

$$J(\sigma_s, h) = \sum_j^{\lambda > 0} V_j \left(V_c(\sigma_s + h/\lambda_j) - V_c(\sigma_s + h/\lambda_j) \frac{h}{\lambda_j \bar{\sigma}_{c,j}} \right) + \sum_j^{\lambda < 0} V_j \left(V_c(\sigma_s - h/\lambda_j) + V_c(\sigma_s - h/\lambda_j) \frac{h}{\lambda_j \bar{\sigma}_{c,j}} \right). \quad (27)$$

Fig. 4 shows the magnetization curves as a function of the applied stress in a series of particular cases considering two phases with positive, λ_1 , and negative, λ_2 , magnetostriction and fractional volumes, V_1 and V_2 , respectively. Different combinations of local magnetostriction constants and fractional volumes have been chosen so that, in all the cases, the macroscopic value of the magnetostriction is $\lambda_s = +0.6\lambda_0$. Nevertheless, some remarkable consequences can be obtained from the results shown in Fig. 4. The remanence increases continuously as the stress is applied so that the effective magnetostriction is considered to be positive. However, the behavior shown in Fig. 4e is the opposite one. For intermediate applied fields, a small applied stress yields a positive increment of the magnetization while

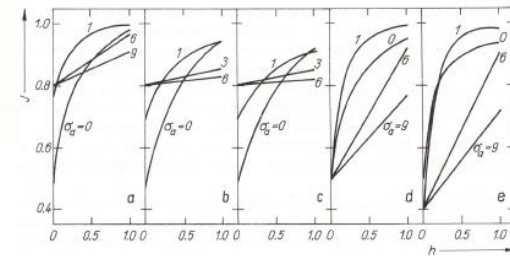
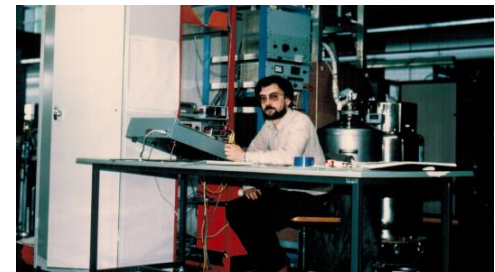


Fig. 4. Magnetization curves for different applied stresses for the case of two phases with positive (λ_1) and negative (λ_2) magnetostriction and fractional volumes V_1 and V_2 , respectively. a) $\lambda_1 = 0.8$, $\lambda_2 = 0.2$, $V_1 = 0.8$, $V_2 = 0.2$; b) $\lambda_1 = 1.0$, $\lambda_2 = 1.0$, $V_1 = 0.8$, $V_2 = 0.2$; c) $\lambda_1 = 1.1$, $\lambda_2 = 1.4$, $V_1 = 0.8$, $V_2 = 0.2$; d) $\lambda_1 = 1.4$, $\lambda_2 = 0.2$, $V_1 = 0.5$, $V_2 = 0.5$; e) $\lambda_1 = 1.8$, $\lambda_2 = 0.2$, $V_1 = 0.4$, $V_2 = 0.6$. Note that in all the cases $\lambda_s = +0.6\lambda_0$.



Exponente crítico de la magnetostricción

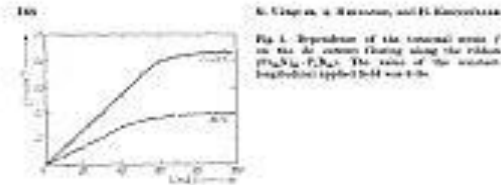


Fig. 1. Dependence of the torsional strain J on the dc current flowing along the ribbon ($F_{10} = 2.0 \times 10^{-3}$ N, $F_{20} = 1.0 \times 10^{-3}$ N). The value of the constant longitudinal applied field was 0.10 T.

sample. The ribbon was vertically placed and fixed at the top. The lower end of the ribbon was clamped on a light aluminum wire (Fig. 2a) which was attached to an electrical bath through the flow of electrical current. While the sample was free to undergo torsional strain. Moreover, the sample was placed within a furnace so that the torsional deflection could be measured also as a function of temperature. The deflection was measured with the help of a small mirror connected with the aluminum tube by means of a laser beam and measuring the displacement of the reflected beam on a scale disposed far away.

The influence of both applied magnetic fields has been discussed recently [7, 8] and the magnetization is roughly given by

$$J = J_{sat} \left(\frac{H}{H_0} \right)^{\alpha} \quad (1)$$

where α is the index of the ribbon and J_{sat} the saturation value of the torsional deflection. J_{sat} is obtained from the experimental $J \sim H$ curve when a fixed longitudinal magnetic field is applied (high enough to produce a linear saturation of the magnetization along its direction and being usually of the order of magnitude of a few kOe (see Fig. 1)).

Two different samples obtained by quenching from the melt were used for measurements. Their nominal compositions are $Fe_{40}Ni_{10}P_{14}B_6$ and $Fe_{40}Ni_{10}P_{14}B_6$. The variation of α with temperature of both samples is shown in Fig. 2.

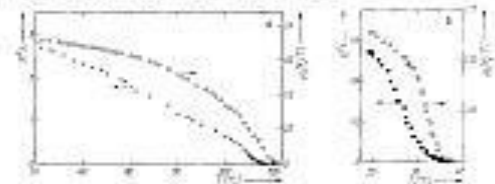


Fig. 2. Temperature dependence of the magnetostriction exponent α of the applied field for (a) $Fe_{40}Ni_{10}P_{14}B_6$ and (b) $Fe_{40}Ni_{10}P_{14}B_6$ alloys.

phys. stat. sol. (a) **115**, 547 (1989)

Subject classification: 75.60; 75.25; S1.1; S1.2; S1.61; S1.62

U.E.I. de Materiales Magneticos, Instituto de Ciencia de Materiales, Madrid¹⁾ (a),
Firma Vacuumschmelze GmbH, Hanau²⁾ (b),
and Institut für Physik, MPI für Metallforschung, Stuttgart³⁾ (c)

Approach to Magnetic Saturation in Rapidly Quenched Amorphous Alloys

By

M. VAZQUEZ (a), W. FERNENGEL (b), and H. KRONMÜLLER (c)

$$\frac{a_1}{\mu_0 H} = 1.1 \mu_0 \frac{G^2 \lambda_s^2}{(1 - \nu)^2} \frac{N b_{eff}}{J_s A_{ex}} D_{dip}^2 \frac{1}{\mu_0 H}.$$

For $\chi_H D_{dip} > 1$, the type $1/H^2$ is predominant being given by

$$\frac{a_2}{\mu_0 H^2} = 0.456 \mu_0 \frac{G^2 \lambda_s^2}{(1 - \nu)^2} \frac{N b_{eff}}{J_s^2} D_{dip}^2 \frac{1}{(\mu_0 H)^2}.$$

A. HERNANDO, M. VÁZQUEZ, V. MADURGA
Laboratorio de Magnetismo, Facultad de C. Físicas, Universidad Complutense, Madrid-3, Spain

and

H. KRONMÜLLER
Max-Planck-Institut für Metallforschung, Institut für Physik, Stuttgart, and Institut für Theoretische und Angewandte Physik der Universität Stuttgart, Stuttgart, Fed. Rep. Germany

Received 23 December 1982

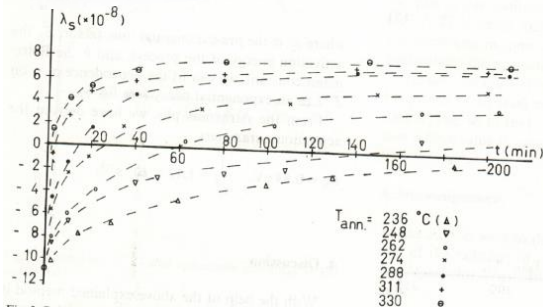


Fig. 3. Relaxation of the magnetostriction constant after different annealing times for a range of annealing temperatures.

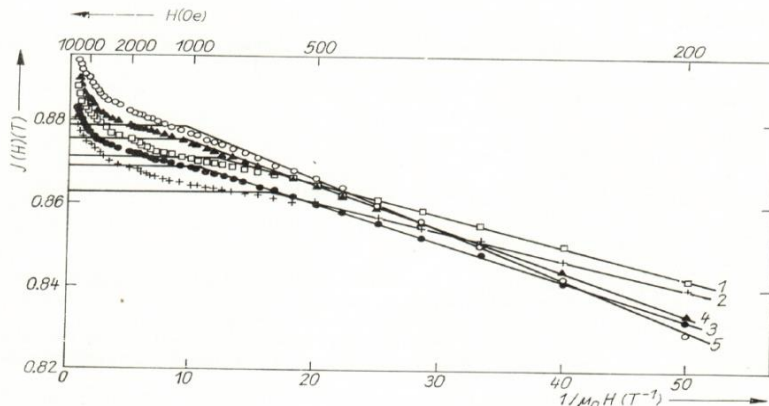


Fig. 3. The magnetic polarization as a function of $1/\mu_0 H$ of the $Fe_{40}Ni_{10}P_{14}B_6$ alloy for the as-cast state (1), after preannealing 2 h at 330 °C (2) and after subsequent thermal treatments: either under transverse magnetic field (3 kOe, 8 h at 240 °C) (3) or under 780 MPa tensile stress at 330 °C during 2 h (4) and 4 h (5).

- Postdoc en Danmarks Tekniske Universitat, Lyngby, Invierno 1984-5 (NATO grant) Magnetostricción e Imanación a saturación

MAGNETOSTRICTION AND OTHER MAGNETIC PROPERTIES OF Co-Ni BASED AMORPHOUS ALLOYS

M. VÁZQUEZ *, A. HERNANDO ** and O.V. NIELSEN

Department of Electrophysics, The Technical University of Denmark, DK-2800 Lyngby, Denmark

Received 4 February 1986; in revised form 20 March 1986

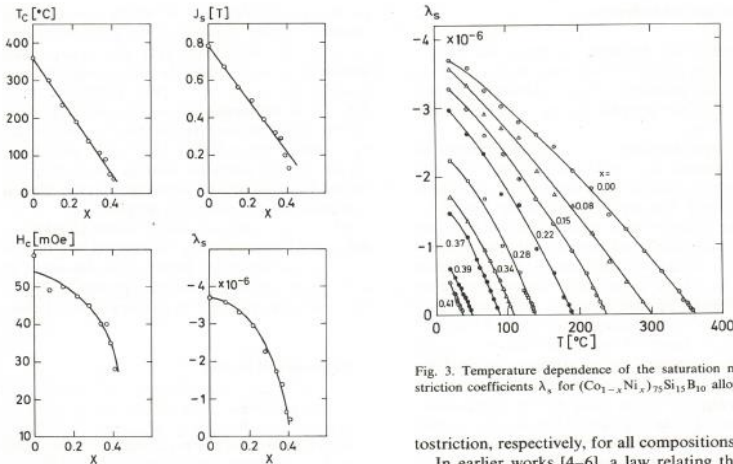


Fig. 1. Curie temperatures T_c , room temperature values of saturation polarization J_s , coercive fields H_c and saturation magnetostriction coefficients λ_s for $(\text{Co}_{1-x}\text{Ni}_x)_{75}\text{Si}_{15}\text{B}_{10}$ alloys.

J. [T]

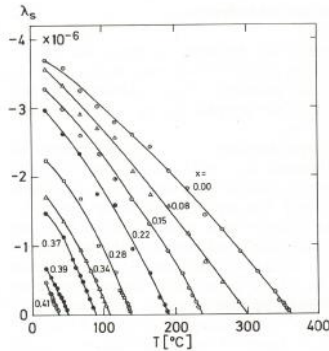


Fig. 3. Temperature dependence of the saturation magnetostriction coefficients λ_s for $(\text{Co}_{1-x}\text{Ni}_x)_{75}\text{Si}_{15}\text{B}_{10}$ alloys.

tostriction, respectively, for all compositions.

In earlier works [4-6], a law relating the temperature dependence of J_s and λ_s was found for Co-Fe and Co-FeNi based amorphous alloys, described by

$$\lambda_s(T) = \alpha [J_s(T)]^3 + \beta [J_s(T)]^2. \quad (2)$$

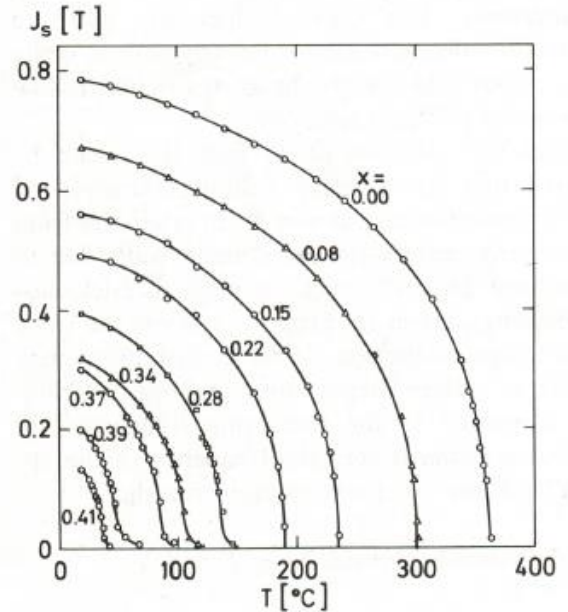


Fig. 2. Temperature dependence of the saturation polarization

$$\lambda_s(T) = \alpha [J_s(T)]^3 + \beta [J_s(T)]^2.$$

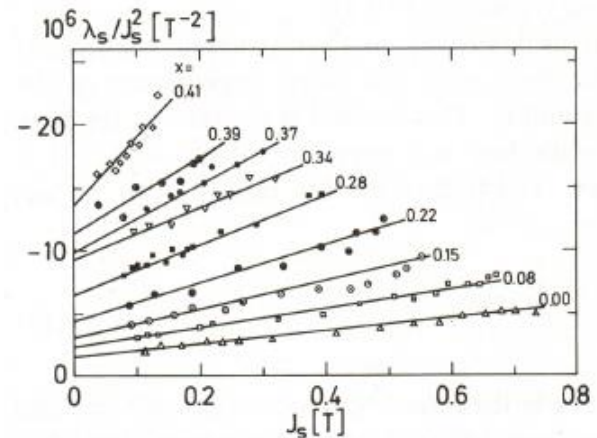


Fig. 4. The data from figs. 2 and 3 fitted to eq. (2) in the text.



cena con Otto Nielsen y Etienne Trémolet du Lacheisserie

Vuelta al Laboratorio de la Complutense, 1985-89

Cintas Amorfas: Anisotropías Inducidas; Magnetostricción; Torsión

Primeras Tesis: Cristina Núñez de Villavicencio; Julian González

A NEW, SIMPLE MEASUREMENT OF THE MAGNETOSTRICTION CONSTANT IN METALLIC GLASS RIBBONS

C. NÚÑEZ DE VILLAVICENCIO *, M. VÁZQUEZ, V. MADURGA and A. HERNANDO

Laboratorio de Magnetismo, Facultad de Ciencias Físicas, Universidad Complutense, 28040 Madrid, Spain
 * *Cátedra de Física Médica, Facultad de Medicina, Universidad Complutense, 28040 Madrid, Spain*

Received 9 October 1985; in revised form 16 December 1985

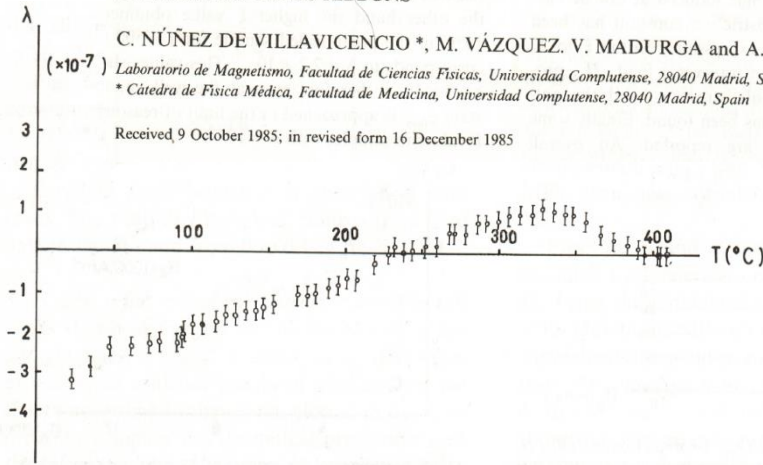


Fig. 10. λ as a function of the temperature T , $H_z = 120 \text{ Am}^{-1}$, $I = 20 \text{ mA}$. Sample 4 $(\text{Fe}_{0.5}\text{Co}_{0.95})_{75}\text{Si}_{15}\text{B}_{10}$.

INDUCED MAGNETIC ANISOTROPY AND CHANGE OF THE MAGNETOSTRICTION BY CURRENT ANNEALING IN Co-BASED AMORPHOUS ALLOYS

M. VÁZQUEZ, J. GONZÁLEZ † and A. HERNANDO

Laboratorio de Magnetismo, Facultad de Ciencias Físicas, Universidad Complutense, 28040 Madrid, Spain

Received 1 July 1985; in revised form 29 July 1985

Efecto de la Torsión Aplicada

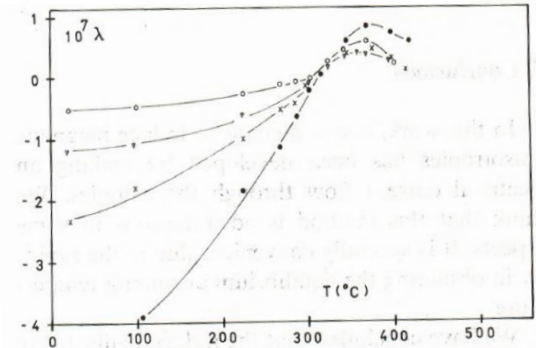
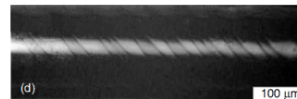
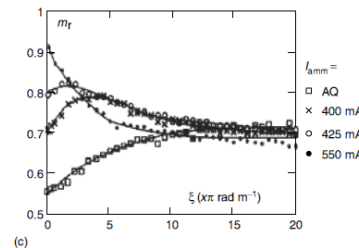


Fig. 7. Dependence of the magnetostriction for the $(\text{Co}_{0.95}\text{Fe}_{0.05})_{75}\text{Si}_{10}\text{B}_{15}$ alloy after current annealing for 180 min at different temperatures [360 mA (●), 440 mA (x), 560 mA (▽), 600 mA (○)].



(b)



(c)

Figure 7. Dependence of switching field on applied tensile stress for a FeSiB in-water-quenched microwire (length = 12, 9.9, 8.4, and 6 cm) (a). (Reproduced from A.M. Severino *et al.*, 1992, with permission from Elsevier. © 1992.) Bitter image of the domain structure at the surface of a torqued microwire (after Hernando *et al.*, to be published), and torsional dependence of remanence for a bistable Fe-based microwire (b). (Reproduced from M. Vázquez *et al.*, 1991, with permission from Elsevier. © 1991.)

$$K_{m,elas}(r) = \frac{3}{2} \lambda_s \mu \xi r$$



Incorporación al CSIC, Serrano 1989-1992

Primeros estudios en microhilos Amorfos y Nanocristalinos

Tesis de Cristina Gomez Polo; Pilar Marín

- Biestabilidad Magnética: Longitud Crítica; Dominios
- Aleaciones Nanocristalinas, Microestructura & Annealings

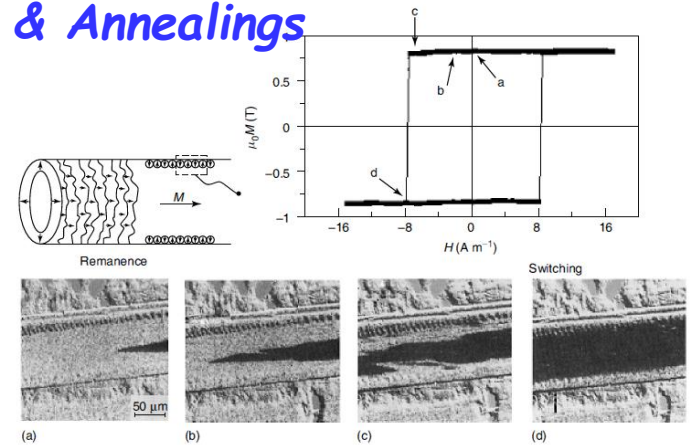
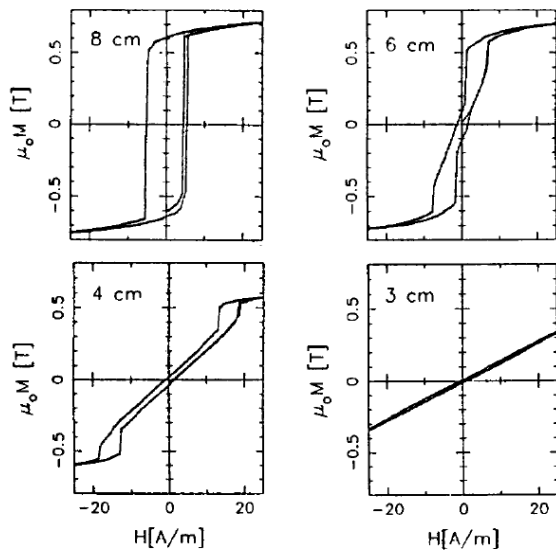


Figure 3. $\text{Fe}_{75}\text{Si}_{15}\text{B}_{10}$ in-water-quenched microwire: correlation between low-field bistable hysteresis loop (top right) and main domain structure (schematic view, top left). Evolution of inner core domain between remanence and switching, as observed by Kerr effect, during magnetization reversal (bottom). (Reproduced from T. Reiningger *et al.*, 1993, with permission from American Institute of Physics. © 1993.)

Fig. 3.- The hysteresis loops for an Fe-rich amorphous wire having different length.



Instituto de Magnetismo Aplicado (1992-2000)

Acuerdo UCM-RENFE-CSIC



Materiales Blandos;
Cintas y Microhilos Amorfos
Nanocristales
Películas delgadas
Sensores Varios
Apantallamiento electromagnético

Excelente experiencia de grupo:

- organización de investigación,
- elaboración de proyectos,
- formación de estudiantes, 8 doctores
- visitantes extranjeros, 12
- colaboración con empresas / patentes



Instituto de Magnetismo Aplicado (1992-2000)

investigadores visitantes



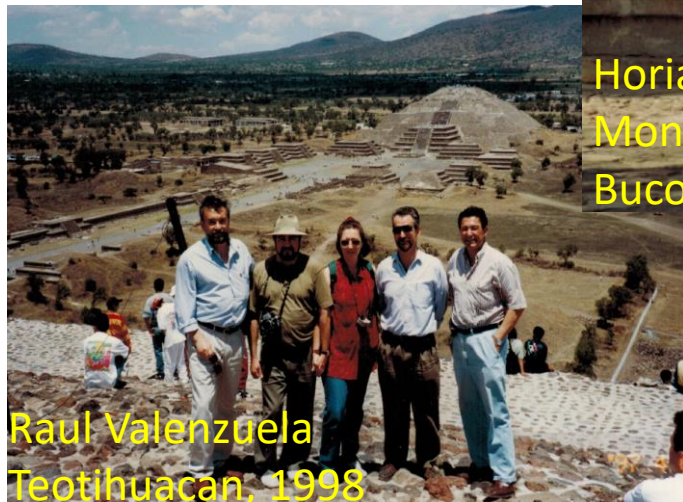
Chen Duxing,
Baltimore 1996



MMM Albuquerque,
1998



Horia Chiriac
Monasterios de
Bucovina, 1992



Raul Valenzuela
Teotihuacan, 1998

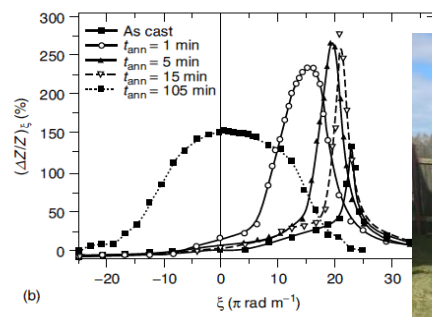
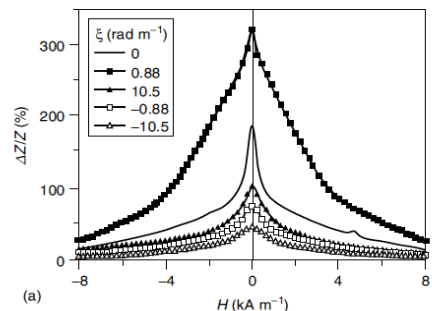
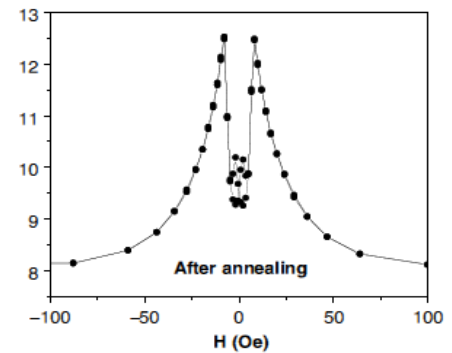
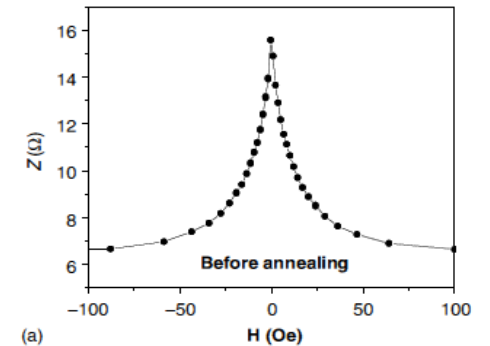
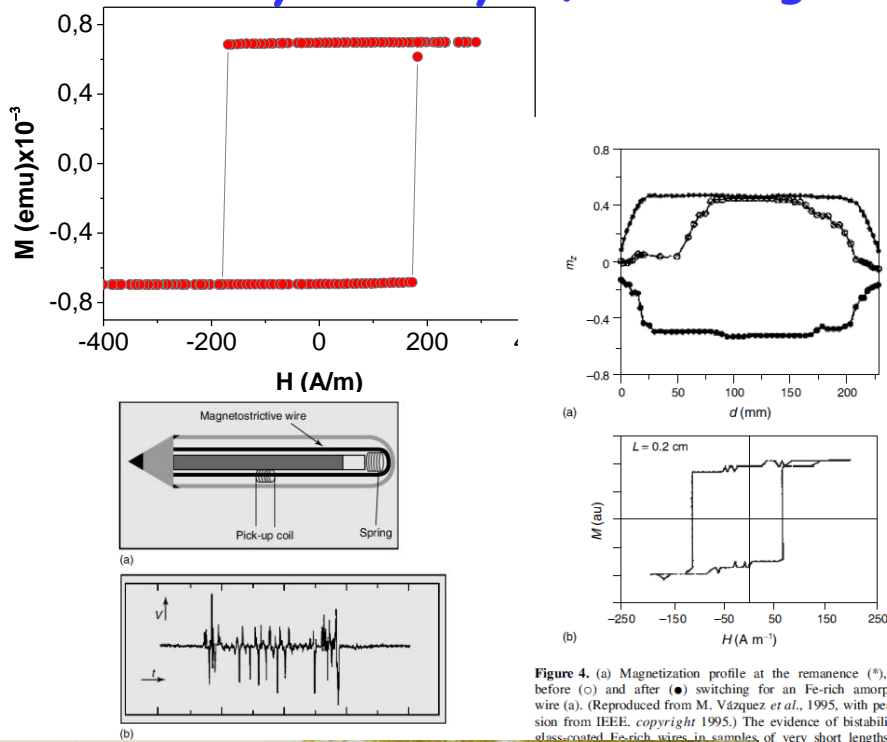


LAW3M,
Sao Paulo, 1996

Instituto de Magnetismo Aplicado (1992-2000)

Arcady Zhukov (Biestabilidad Magnética, alta magnetostricción, sensores)

Galina Kurlyandskaya (Giant Magnetoimpedance, magnetostricción cero)



Single peak (a) and two peaks (b). GMI behavior



Con A. Zhukov, G. Kurlyandskaya Ekaterinburg, 1998



Figure 19. Evolution of magnetoimpedance response microwire under applied torque (a). (Reproduced from *et al.*, 2003, with permission from the American Institute of Physics. © 2003.) Asymmetric torsion impedance after a helical anisotropy is induced by torsion annealing (b). (Reproduced from M. Vázquez *et al.*, 2003, with permission from Elsevier. © 2003.)

Visitas/Conferencias Internacionales



Benalmádena, 1986



Balaton, Hungría, 1987



Visitas Anglo-Españolas, 1992

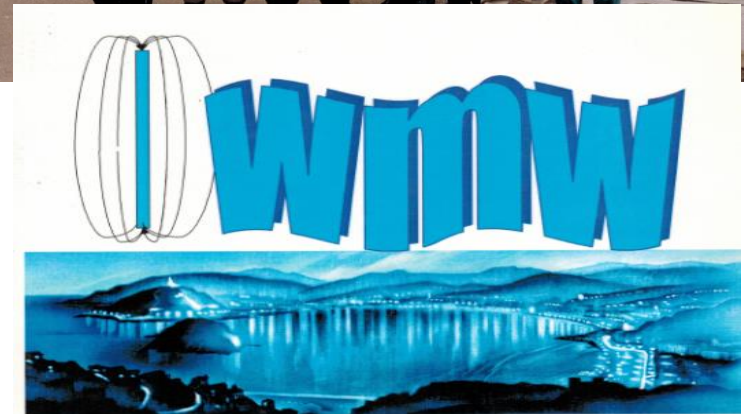


Promotores del EMSA, 1994

IV International Workshop on
Non-Crystalline Solids

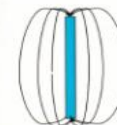


Organized by
Instituto de Magnetismo Aplicado
Expo-Chamartin
MADRID, SPAIN
20th-23rd September 1994
BOOK OF ABSTRACTS



INTERNATIONAL WORKSHOP ON MAGNETIC WIRES

San Sebastian (Spain), June 20-23, 2001



Organized & Sponsored by:
Ministerio de Ciencia y Tecnología
Consejo Superior de Investigaciones Científicas
Universidad del País Vasco
Universidad Pública de Navarra
Gobierno Vasco
Excmo. Ayuntamiento de San Sebastián

Instituto de Ciencia de Materiales (2001 -2008)

Formación de un Nuevo Laboratorio/Grupo

Aspectos a tener en cuenta para alcanzar contribuciones originales:

- Producción autónoma de muestras
- Medidas experimentales originales
- Personal investigador

**Finanzas: solicitar fríamente
todo tipo de proyectos**



Líneas de Investigación:

Microhilos:

Arcady Zhukov, Rastislav Varga; Giovanni Badini-Confalonieri

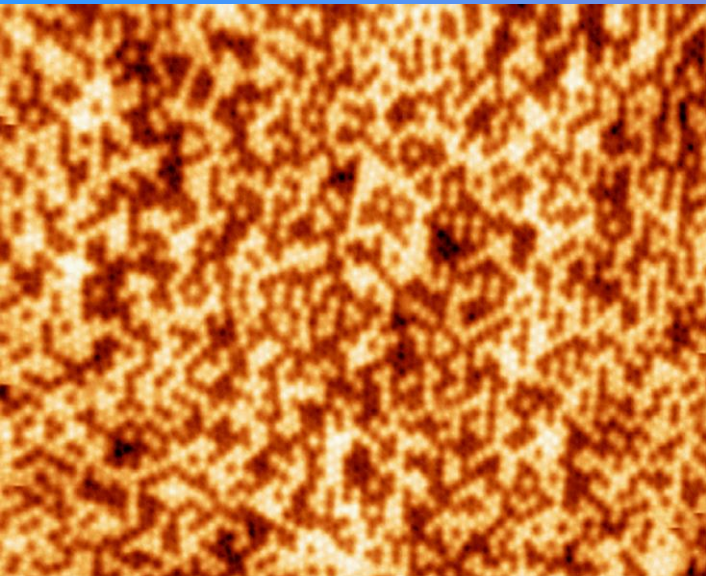
Nanohilos:

Kornelius Nielsch; Manuel Hdez-Velez; Kleber Pirota; Victor Prida

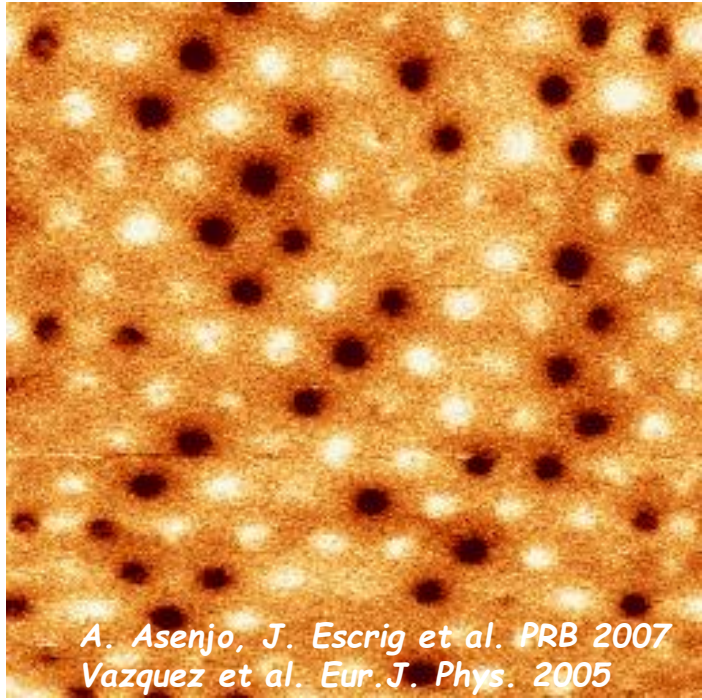
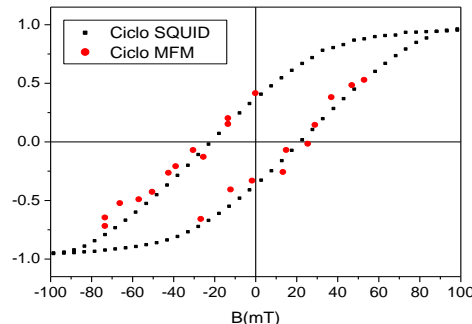
Magnetismo de Superficie, MFM:

Agustina Asenjo

Hysteresis loops & Spin imaging: VSM & SQUID vs. VF-MFM & MTXM



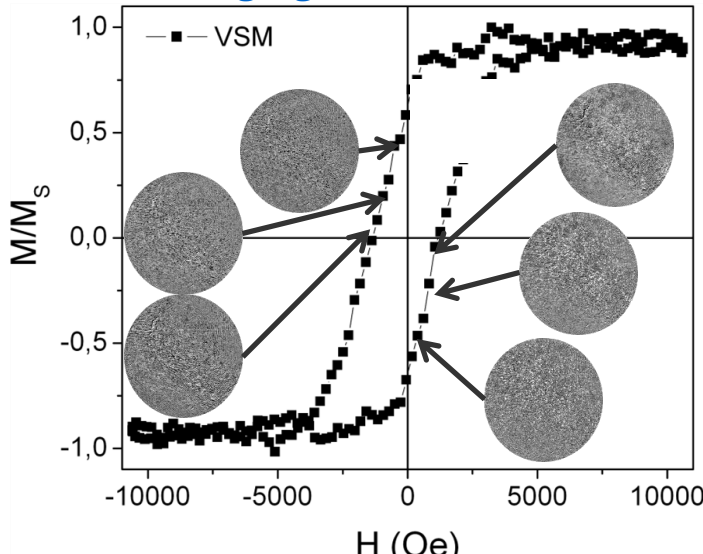
MFM imaging of Ni nanowires
($d=180$ nm, $L = 2$ μ m)



A. Asenjo, J. Escrig et al. PRB 2007
Vazquez et al. Eur.J. Phys. 2005

Evidence of Magnetostatic Interactions

MTXM imaging of Co nanowires ($d=35$ nm, $L=150$ nm)



Miriam

Advanced Light Source,
Berkeley
MTXM: line 6.1.2;
Co edge (778 eV)
Collaboration P. Fischer
Open Surf. Sci.

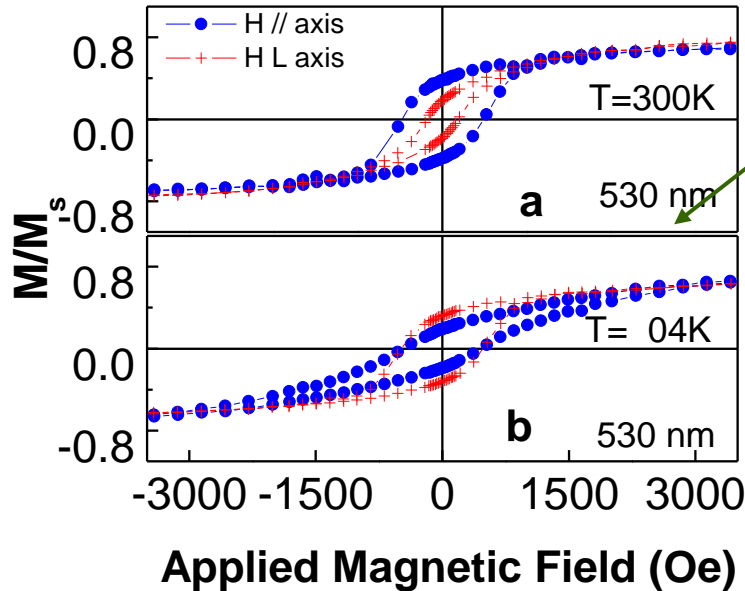
Unexpected temperature dependence of Magnetic Anisotropy

Arrays of Ni, Co Nanowires with different length (500 to 2000 nm)

in collaboration with
Un. Campinas (M. Knobel)

David Navas

Change of magnetoelastic contribution with temperature

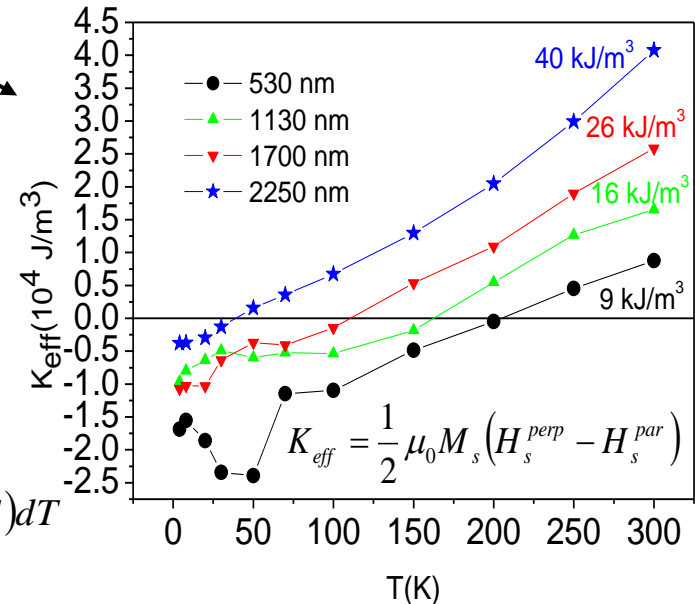


Change of Anisotropy
Axis with
Temperature!!

The crossing
temperature depends
on wires length

$$K_{tot} = K_{shape}(L) + K_{mag.el.}(\sigma) + K_{cryst}$$

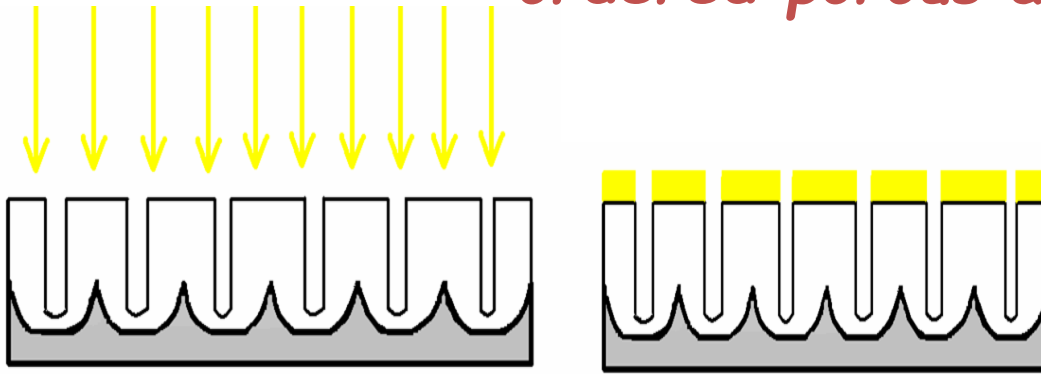
$$K_{\sigma}(T) = \frac{3}{2} \lambda_s(T) \sigma(T) = \frac{3}{2} \lambda_s(T) E_{eff}(L) \frac{\Delta l}{l}(T) = \frac{3}{2} \lambda_s(T) E_{eff}(L) \int_{T_i}^{T_f} \Delta \alpha(T) dT$$



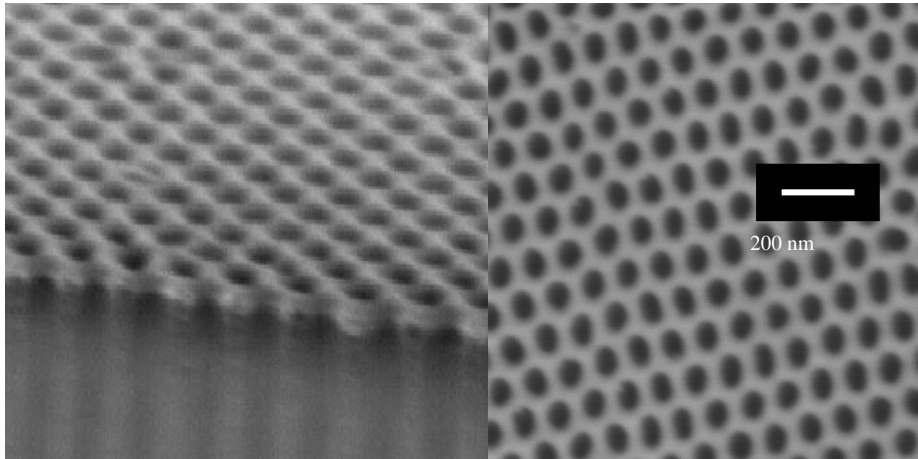
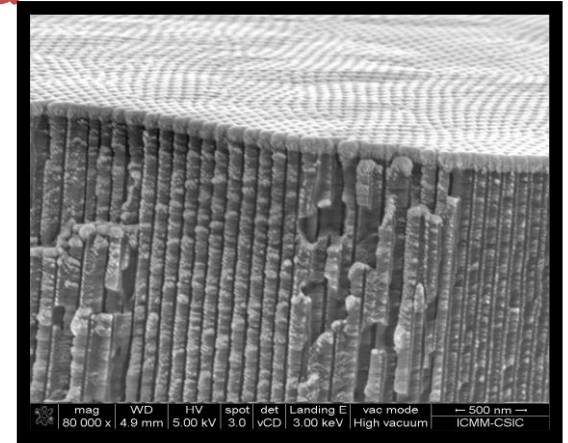
Pirota et al. Phys. Rev. B 76(2007)233410
Navas et al. J. Appl. Phys. 103(2008)

Strong influence of magnetoelastic anisotropy induced by:
a) Different thermal coefficients of wires & matrix
b) Length dependent Young's Modulus (surface tension)

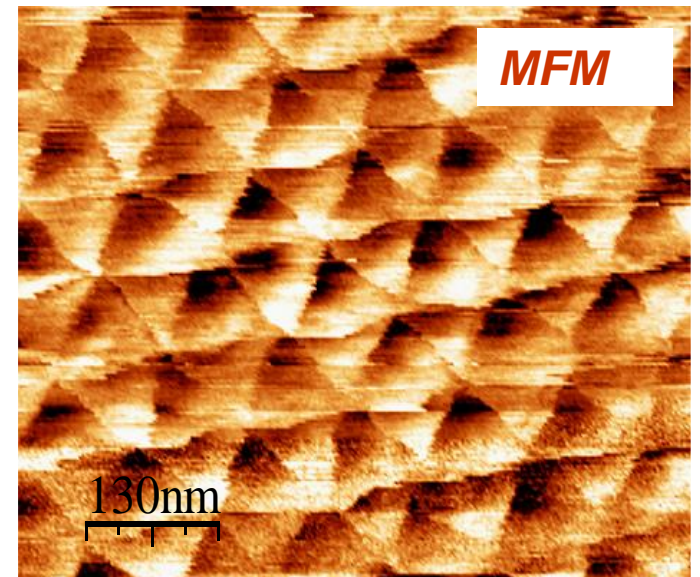
Antidot Py array preparation by ion-beam sputtering on ordered porous alumina



$D=105\text{ nm};$
layer thickness $\approx 20\text{ nm}$ Holes
Length $\approx 4\ \mu\text{m}$



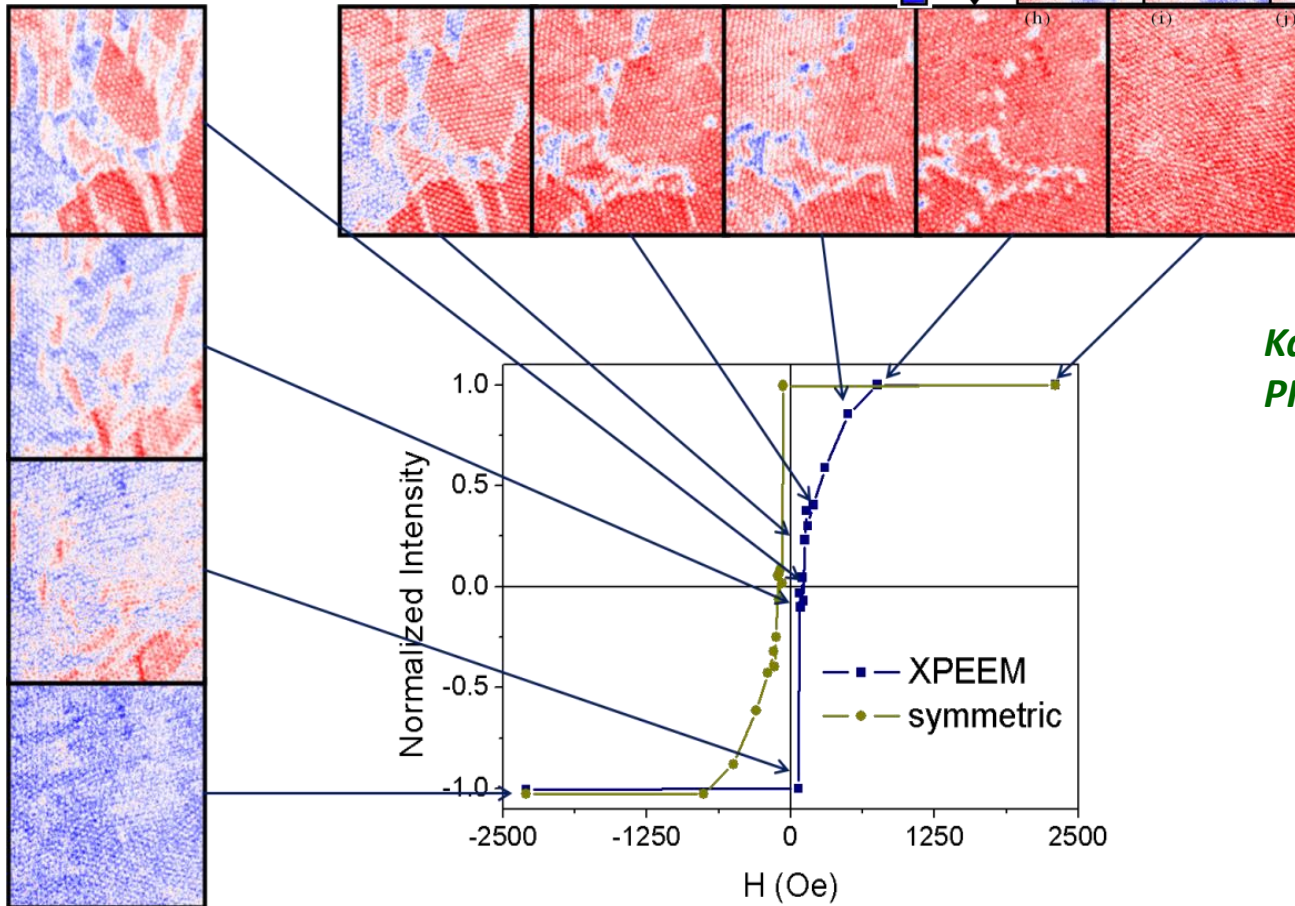
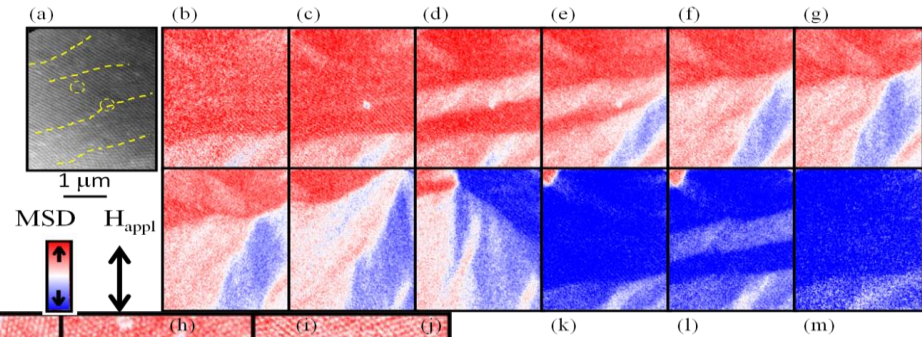
Py antidot array on self-assembled template



Karla, Wagner

Py Antidot Arrays by X-Ray photoemission electron microscopy

XPEEM equipment
at BESSY II synchrotron, Berlin



Karla J Merazzo et al
PRB 85 (2012)184427

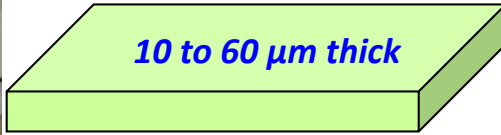
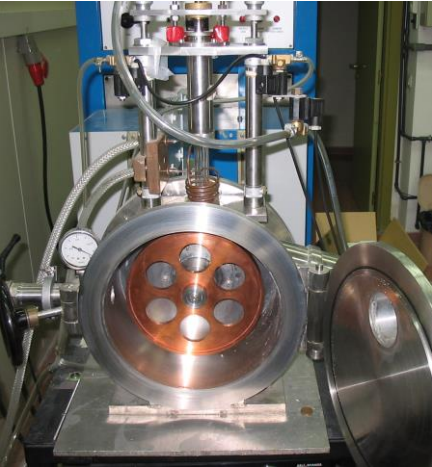
Instituto de Ciencia de Materiales (2001 -) Puesta a punto de un Nuevo Laboratorio



***3 equipos de solidificación ultrarápida:
hilos, cintas y microhilos cubiertos de pyrex***

Families of Metallic Glasses (as produced in ICMM/CSIC, Madrid)

Melt-spun amorphous ribbons



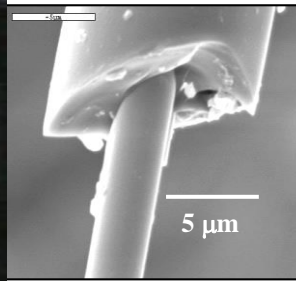
In-water-quenched amorphous wires



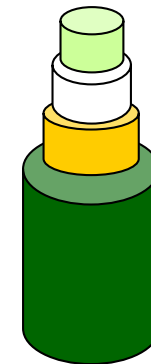
Glass-coated amorphous microwires



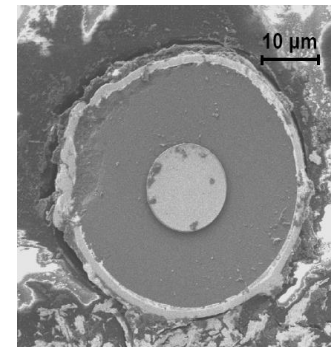
1-20 μm diameter



Up to 40 μm diameter



Bi-magnetic Microwires



Domain Wall & Dynamics

Rastislav Varga; Giovanni Badini-Confalonieri (Karin, Jacob, Germán)

Single domain wall & fundamental dynamics studies

DW motion equation

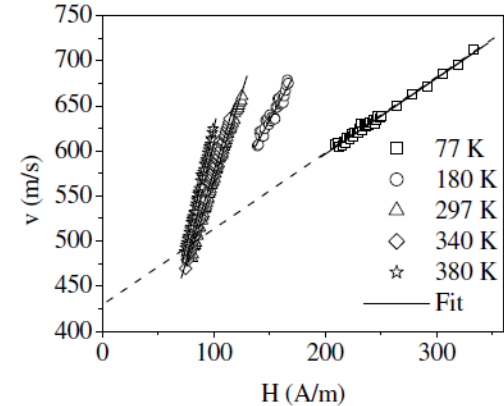
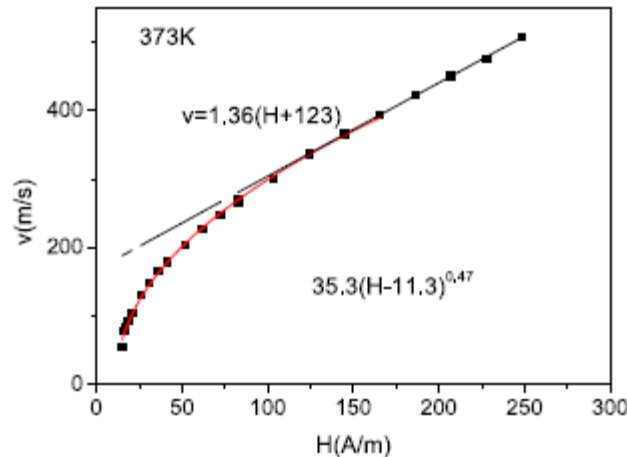
$$m\ddot{x} + \beta\dot{x} + \alpha x = 2M_s H$$

Damping mechanisms

$$\beta = \beta_e + \beta_r + \beta_s = \frac{k_1 M_s(T)^2}{\rho(T)} + k_2 [M_s(T)^3 (1 + r\Delta T)]^{1/2} + k_3 \frac{\tau}{T}$$

Varga et al.
Phys. Rev. Letters 94 (2005) 017201

$$v = S(H - H_0)$$



β_e - eddy currents

β_r - spin relaxation

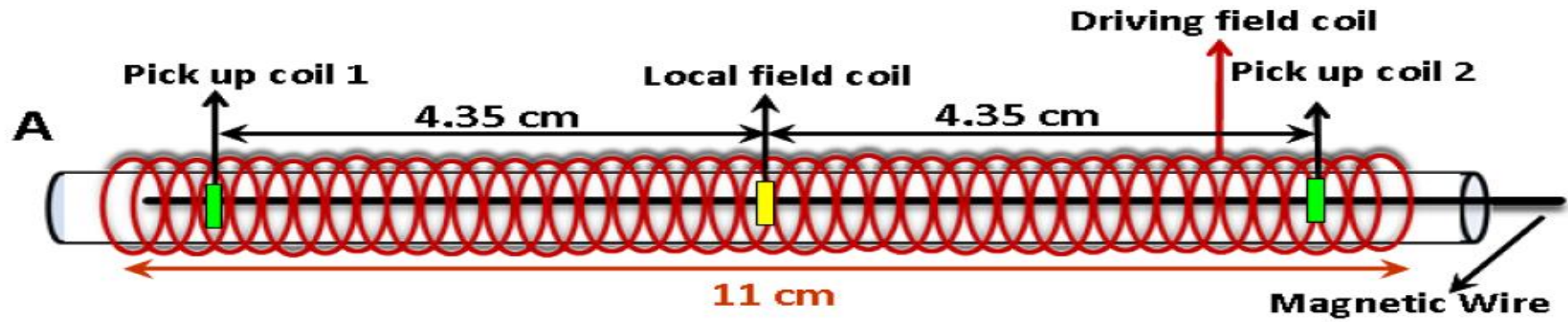
β_s - structure relaxation

$$v = S'(H - H'_0)^\beta$$

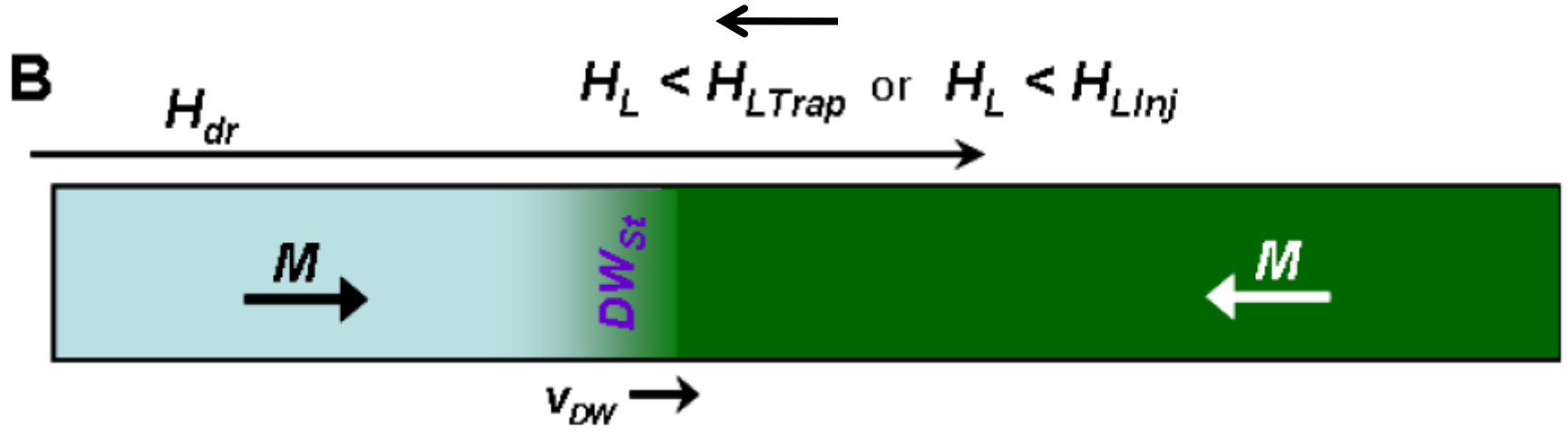
β would reflect the interaction DW with defects

Varga et al.
J. Phys.: Condens. Matter 20 (2008) 445215

Trapping and Injecting Domains Walls: Sixtus & Tonks-like Experiment



Antiparallel local-field configuration:
 The Local field opposes the Drive field

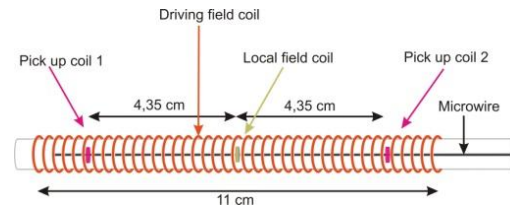
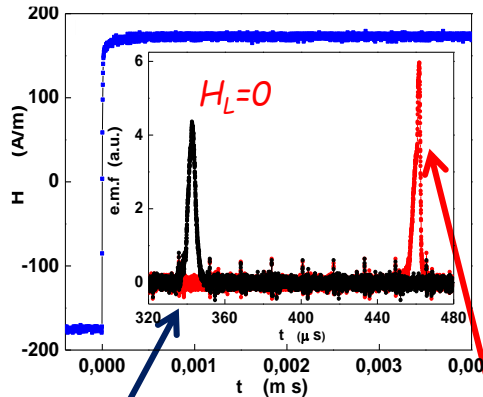
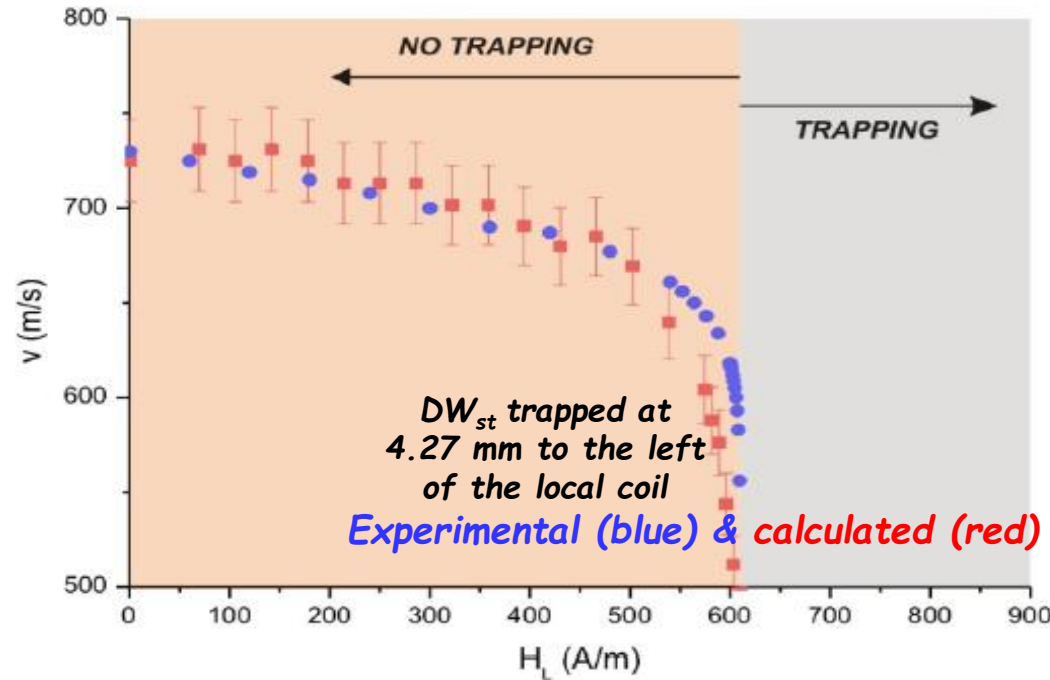


Scheme of domain structure after a standard Domain Wall, DW_{st} , moves under drive field, H_{dr} , plus antiparallel local field

Trapping a domain wall: Antiparallel local-field configuration

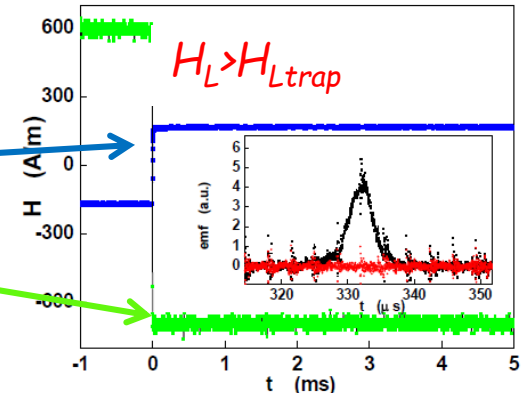
Velocity, v , of the standard wall, DW_{st} , under drive field $H_{dr} = 170$ A/m, as a function of the antiparallel local field, H_L .
The wall gets trapped at $H_L = 610$ A/m

$$mv \frac{dv}{dx} + \beta v + kx = 2\mu_0 M_s S (H_{dr} + H_L(x))$$



Drive field

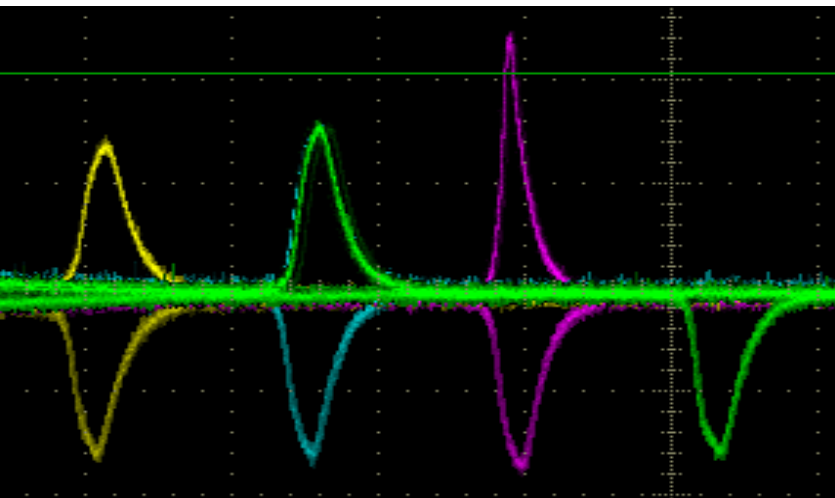
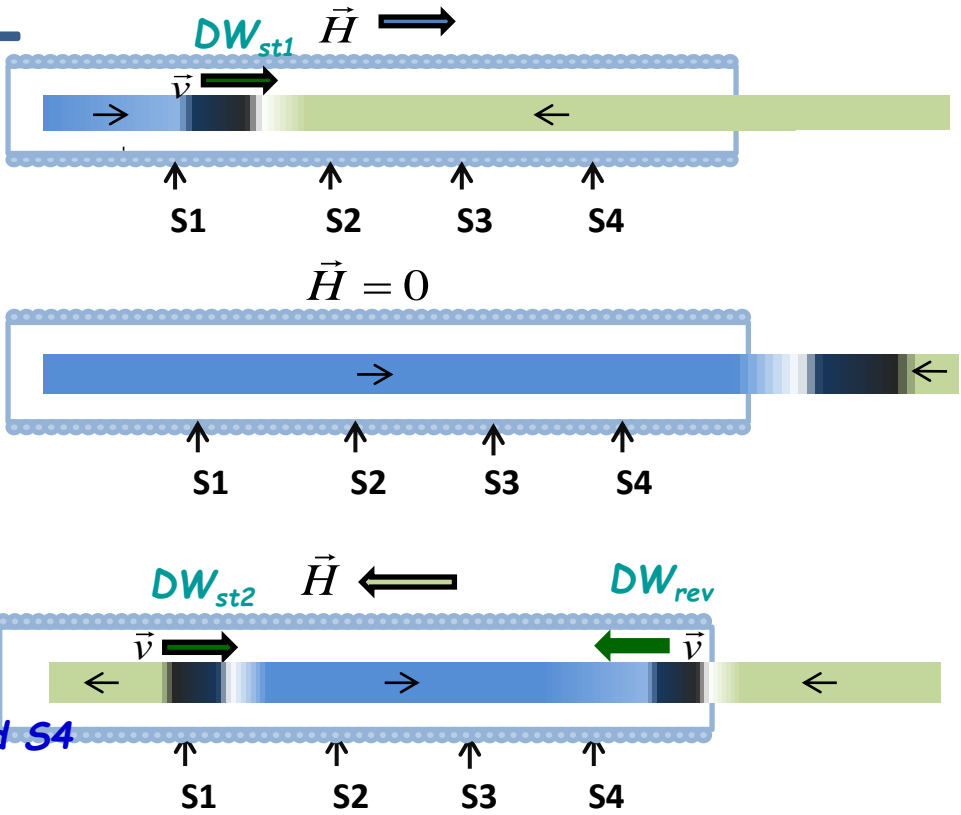
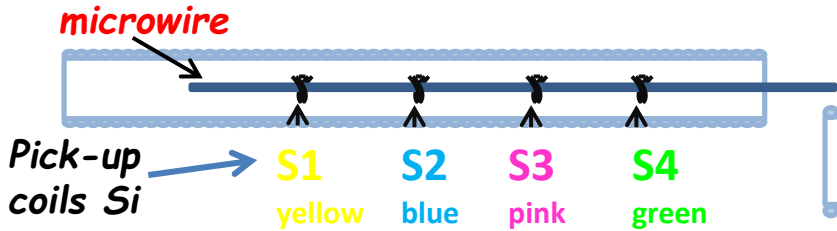
Local field



Vázquez, Basheed, Infante and Perez
Phys. Rev. Letters 108,037201 (2012)

Observando cómo se aniquilan 2 paredes moviéndose en direcciones opuestas

Fe₇₉Si₁₀B₈C₃ microwire
($d_{met}=20.5 \mu m$, $D_{tot}=30.5 \mu m$)



For $H_{app} = -281 \text{ A/m}$, signals at S2 (blue) and S4 (green) are picked up simultaneously.

Also, signal in S3 (pink) has higher amplitude and reduced width.

DW_{st2} and DW_{rev} arrive to S3 simultaneously:

We are observing the collapse of two single domain walls moving along opposite directions

A. Jimenez, R. Perez del Real and M. Vázquez,
 invited talks at JEMS Sept. 2012, Parma (EPJ 2013)
 and at MMM, Jan. 2013, Chicago

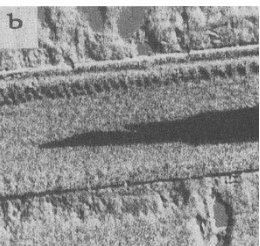
Know-how at ICMM/CSIC: Magnetic Nano and Microwires

1- Materials Production at Laboratory scale



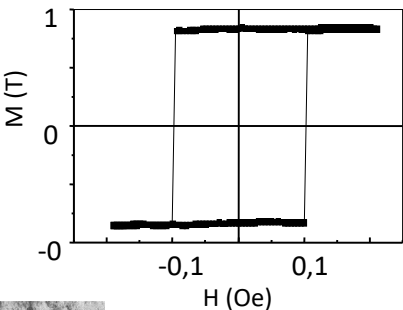
Melt-spinning unit under controlled atmosphere, ICMM/CSIC

Production & Magnetics amorphous ribbons



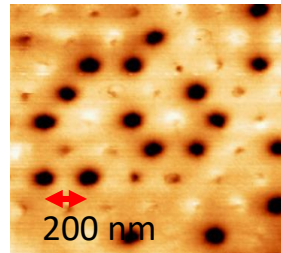
Amorphous Wire Domain structure

Amorphous wires (in-rotating-water)

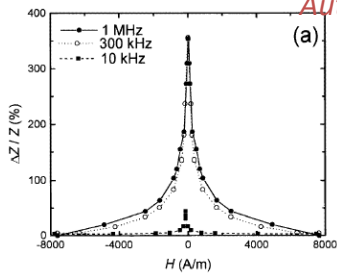


First studies in glass-coated microwires

MFM image of Ni nanowire array



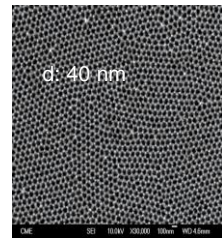
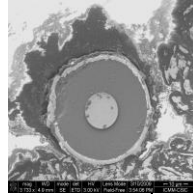
Arrays of Magnetic Nanowires Autonomous Fabrication



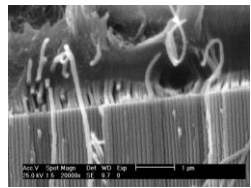
Reporting Giant Magnetoimpedance in amorphous microwires

Autonomous Fabrication of Amorphous Wires and Microwires

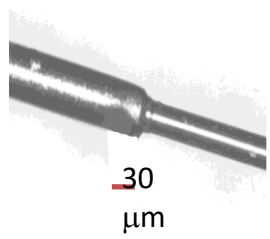
Bimetallic bimagnetic / microwires



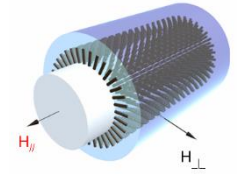
Metallic & Polymeric nanoporous membranes



Radial array of nanowires



Multilayer Microwires



1980-1900

1989

1993

1994-6

2002

2005

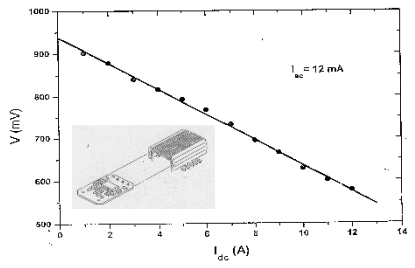
2006

2007

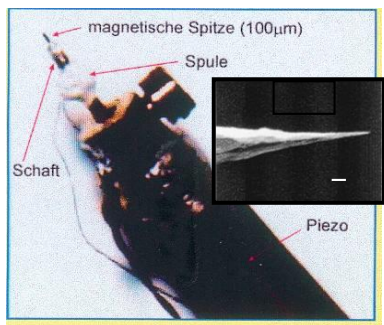
2008

Know-how at ICMM/CSIC: Microwires and sensing devices

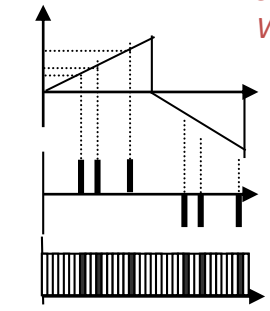
2.- Wire Sensor & Technological Developments



DC current sensor based on MI (Unitika wire) for power electronics

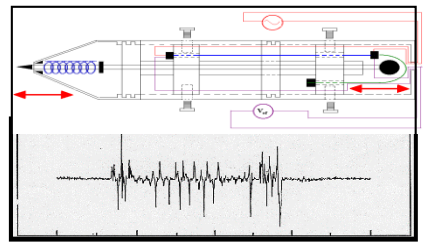


Sharpned Amorphous Wire Tip for SPMTM



Magnetic Encoding based on bistable glass-coated microwires

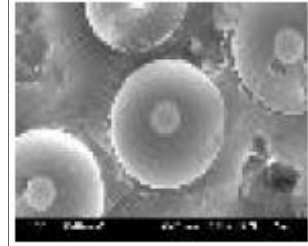
Magnetoelastic Pen for Signature Identification
MI in glass-coated microwire (Patent)



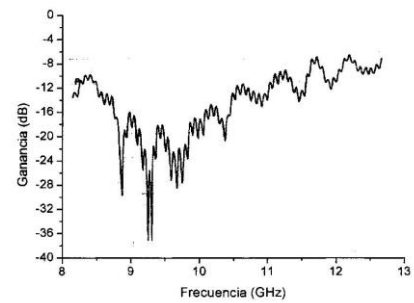
Bimetallic Wire with helical anisotropy (Patent)

Magnetic Shape Memory Wires (Patent)

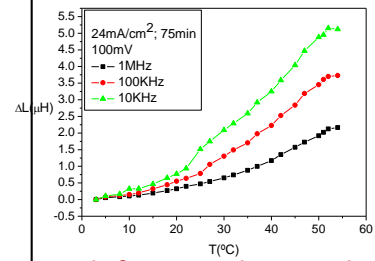
Microwires for Flux-Gate sensor (Quantec Geotech, Montreal)



New-generation 1 micron-size Wire for GMI sensor (Aichi, Toyota Group)



Glass-coated Microwires in polymeric films for electromagnetic screening



Multifunctional Sensor based on Multilayer Microwire (Patent)

1996

1997

1999

2000

2003

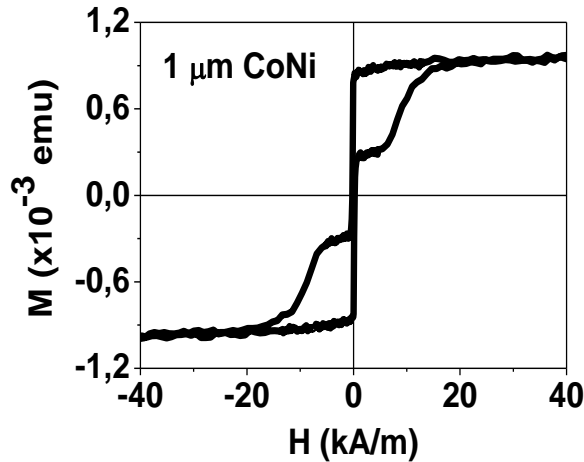
2006

2007

2008-9

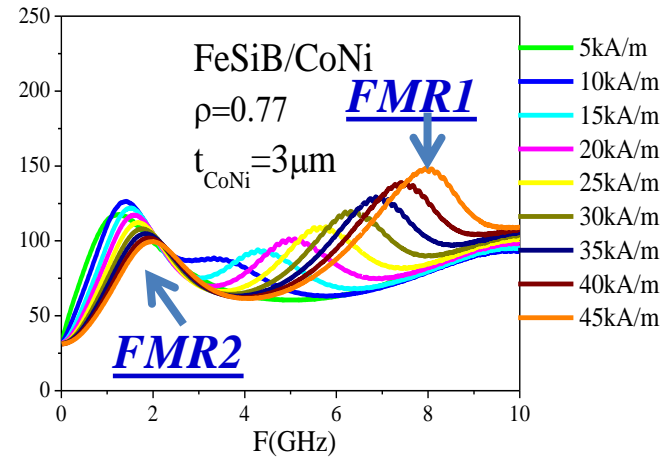
6 Patents based on Multilayer Microwire

FeSiB/CoNi (Soft/Hard)



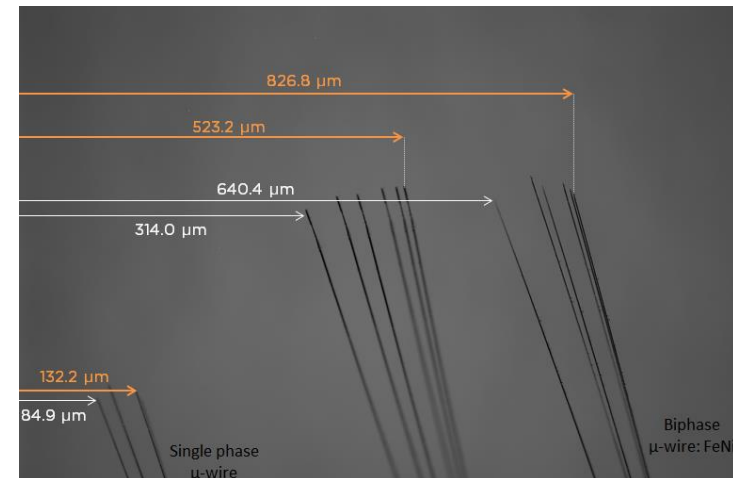
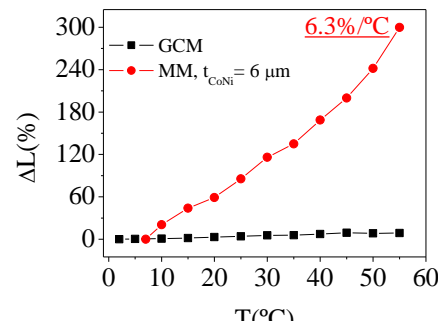
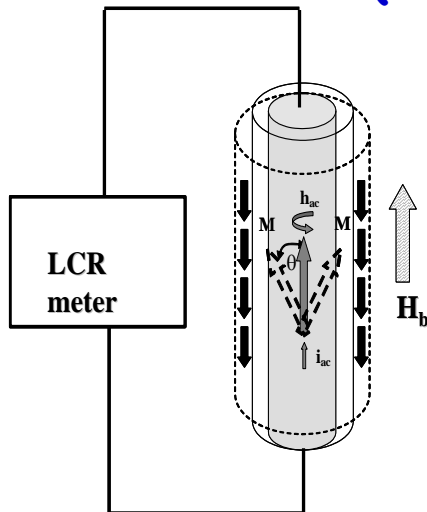
FMR absorption

Rhimou ElKammouni



Temperature & Stress sensor (EU)
 G. Badini, J. Torrejon, K. Pirola,
 H. Pfützner et al. (2007)

Microactuator based on bimagnetic
 asymmetric core/shell microwires (2017)
 EU/Russia (Valeria Rodionova)



*Instituto de Ciencia de Materiales (2001 -)
Organizacion de Congresos, Intermag 2008*



con los Nobel Peter Grünberg y Albert Fert, y la ministra Cristina Garmendia



Instituto de Ciencia de Materiales (2008-2017)

Visitas de investigadores y Distinguished Lecturers



M. Yamaguchi



O. Kazakova



S. Parkin



L. Schultz & R. Cowburn



H. Ohno



NMP, Mittal, Karagpur



Un. Kosiçe



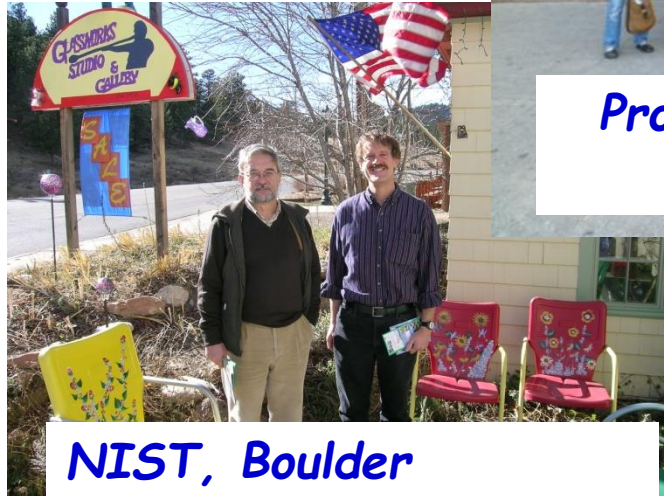
AICHI steels, Toyota



Relaciones Internacionales (2008-2017)



Proyectos Coordinados Españoles



NIST, Boulder

IBM, Almaden, CA

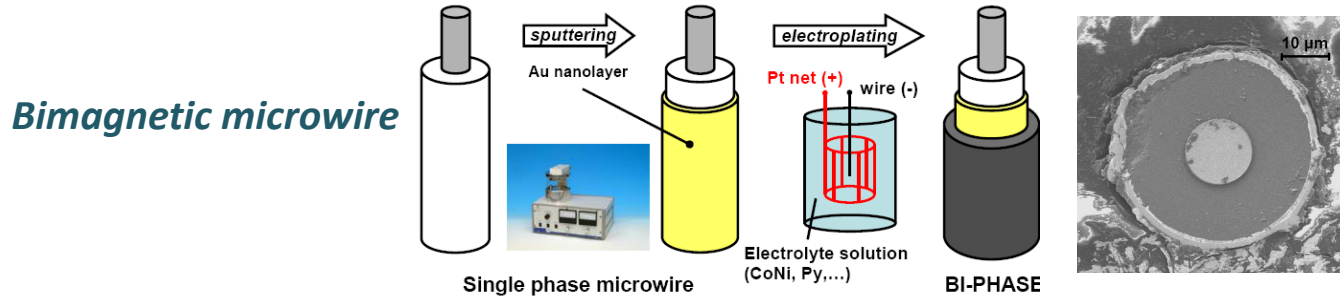


Instituto de Ciencia de Materiales (2009-2017)
Grupo de Nanomagnetismo y Procesos de Imanación

- *Magnetismo de Microhilos:*
control sobre paredes individuales
- *8 Patentes: sensores diversos,*
diseño de nuevos microhilos
- *Proyectos con empresas*
Aichi (Japón), IBM (USA), Micro-Epsilon Messtechnik (Germany),
Quantec Geotech (Canada), AIRBUS (France), PREMO (Spain)
- *Suministro de microhilos & proyectos*
(Un. Pub. Navarra, ...)

Coordinated European Projects

“**Magnetstrictive bi-layers for multifunctional sensor families**” 2003-2007 EU-Growth IPs: H. Pfützner (Techn. Un. Vienna), M Vazquez (CSIC), Cardiff Un. (T. Moses), Fiat (J.Chiricco), ELCAT (Germany).



- “**Magnetic nanoparticles combined with submicron bubbles for oncology imaging (NANOMAGDYE)**” 2008-2012, FP7-NMP-2007; IPs: G. Pourroy (CNRS, Grenoble), I. Bernhard (Saarland Un.), M. Vázquez (CSIC), P. Chirico (Softech, Italy), P. Vertesy (Hungarian Ac. Sc.)

- “**Rare Earth Free Permanent Magnets (REFREEPERMAG)**”, 2012-2016 FP7NMP.2011 IPs: D. Niarchos (NCRS, Athens), M. Vázquez (CSIC), M.Farle (Univ. Duisburg-Essen), J.Fidler (Techn. Un. Vienna), O. Erikson (Un. Uppsala), S. Fähler (IFW, Dresden), F.Ott (CEA, France), G. Viau (Un. Toulouse), Magnetfabrik Bonn, Wittenstein Cyber Motor.



**Position Sensor &
Tachometer**

*Instituto de Ciencia de Materiales (2009-2017)
Grupo de Nanomagnetismo y Procesos de Imanación*

Magnetismo de Nanohilos aislados

Cristina Bran

Agustina Asenjo; Rafael P del Real; Oksana Chubykalo-Fesenko

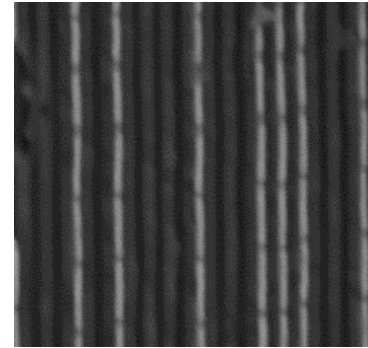
Diferentes tipos de Nanohilos



Various families of magnetic nanowire arrays prepared by electrochemical route at ICMM/CSIC, Madrid

1.- Uniform Nanowires:

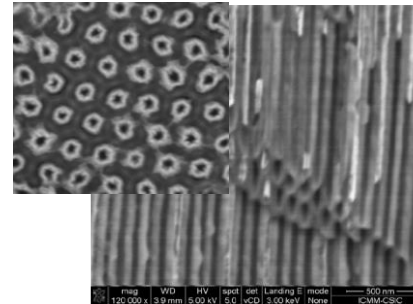
Nanodots, Nanowires
(reduced diameter, combined with ALD)



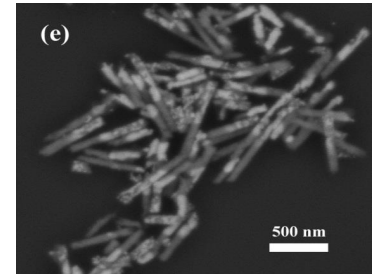
Co/Cu
multisegmented

2.- Modulated Nanowires :

a) Longitudinal
Multisegmented, Multilayer,



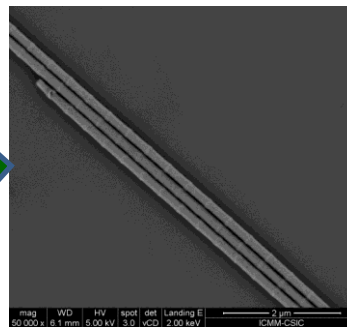
Ni nanotubes



Fe&Au core&shell

b) Radial
Nanotubes, Core/Shell

c) Diameter Modulated

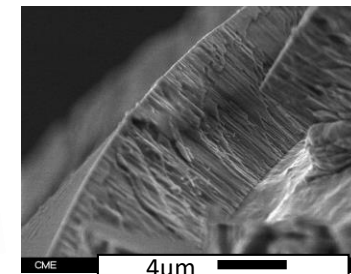
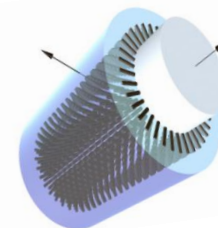


CoFe diameter
modulated

Co nanowires

3.- Radial nanowires in Cylindrical template

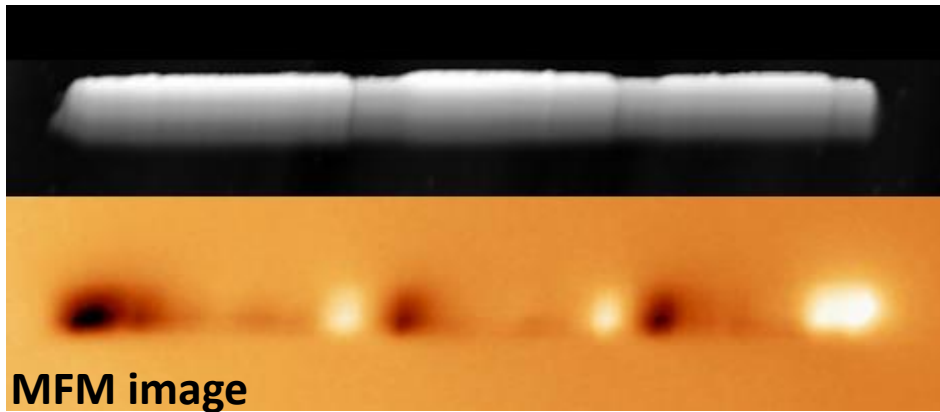
Ruy



Tailored Geometry & Composition (Co, Fe, Ni & alloys)

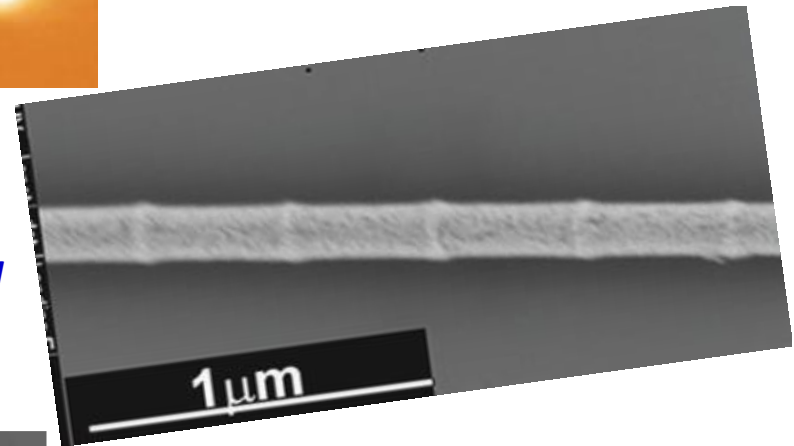
20 to 200 nm Diameter
100 nm to 40 μm Long

Nacho, Oscar

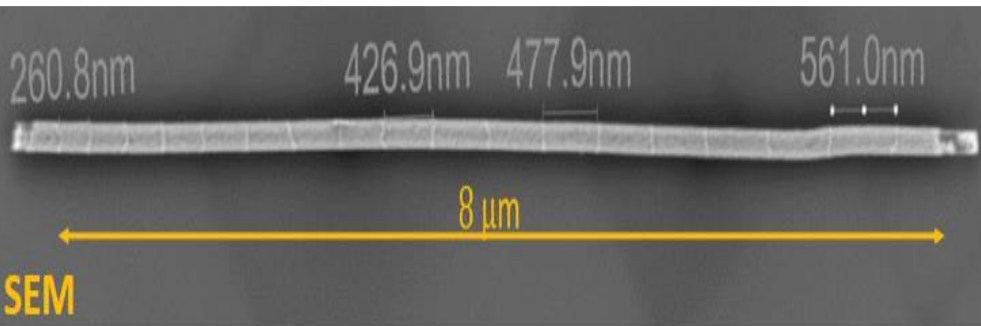


FeCo Diameter- modulated

*FeCo/Cu Bamboo-like
(antinoches) modulated*

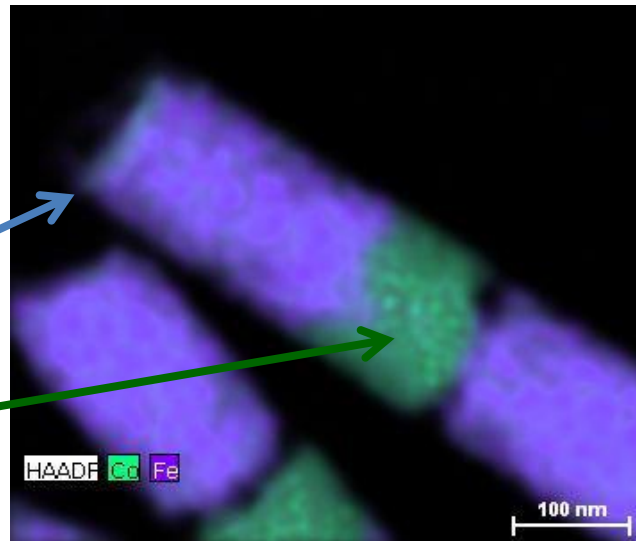


*Multisegmented FeCo/Cu
with increasing FeCo
segment length*

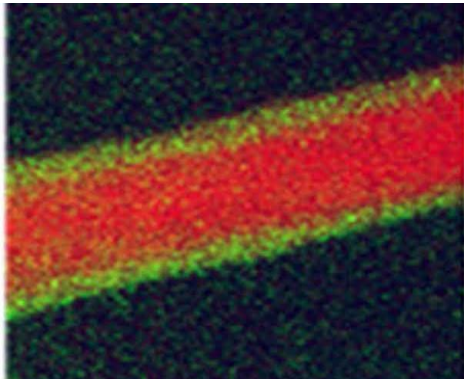


CoFe (bcc 110)

Co (hcp 002)



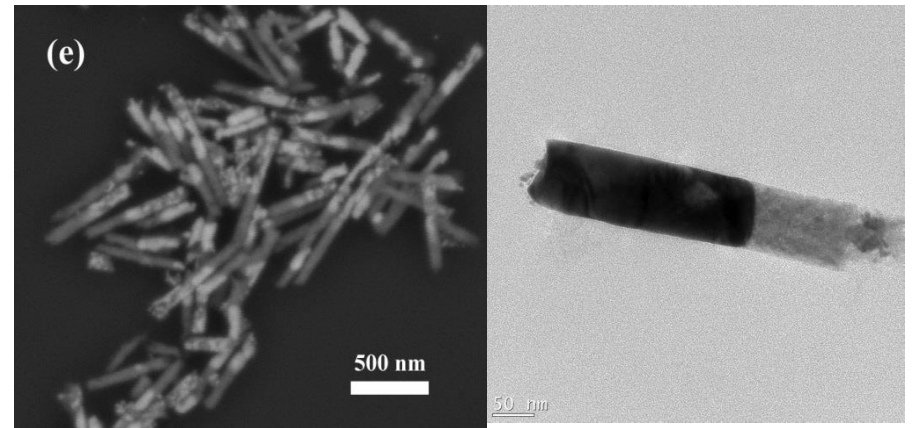
Anisotropy & Composition modulated



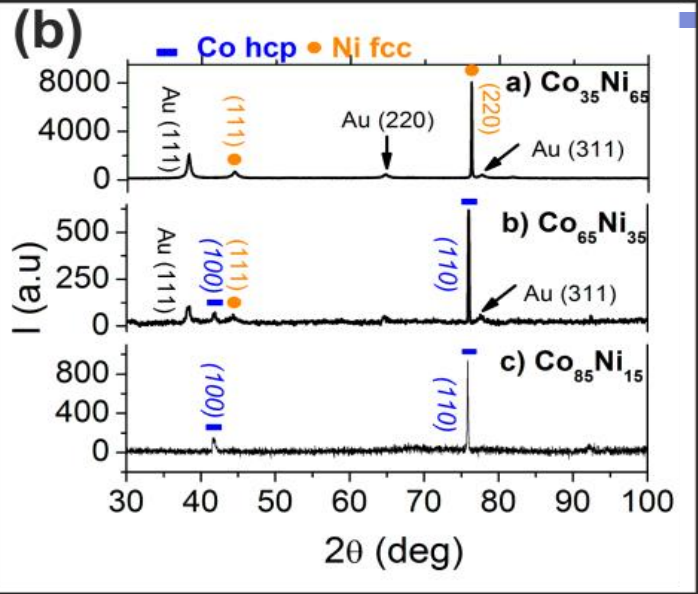
Fe/Fe₃O₄ core/shell nanowire (KAUST)

Yuri Ivanov, Jurgen Kosel (KAUST)

Fe/Au core/shell nanowires

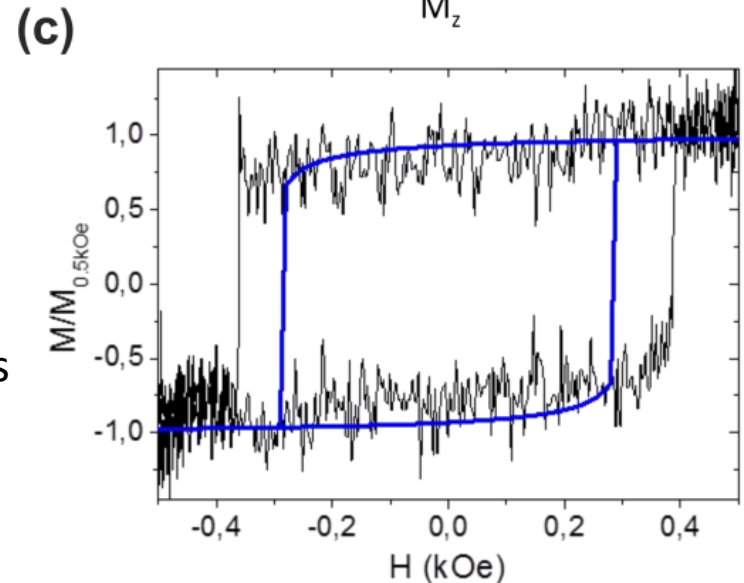
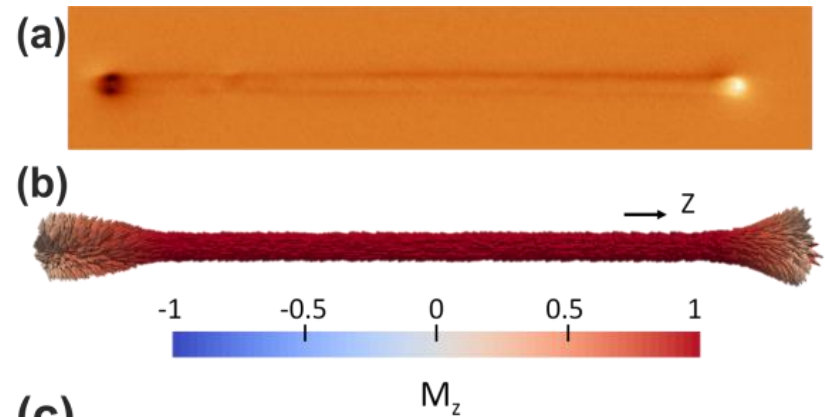


Crystal Structure; Domain Structure; Magnetizat. Reversal



$\text{Co}_x\text{Ni}_{(100-x)}$ allow nanowires

Single Domain in fcc $\text{Co}_{35}\text{Ni}_{65}$

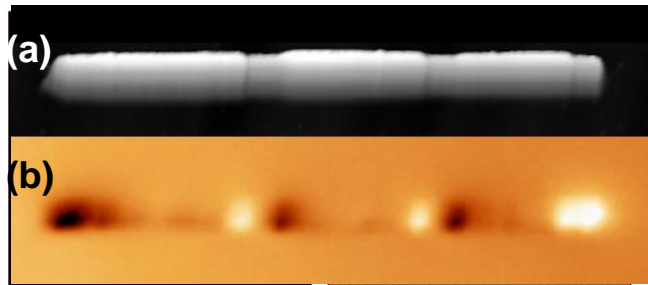


(a) MFM image,

(b) Remanence: micromagnetic simulated

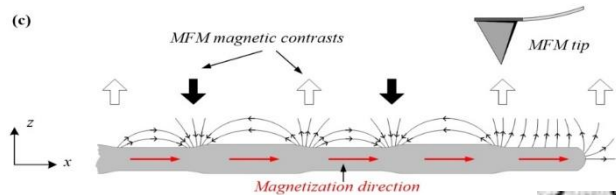
(c) MOKE (black) and simulated (blue) loops

Magnetic Force Microscopy & Electron Holography imaging

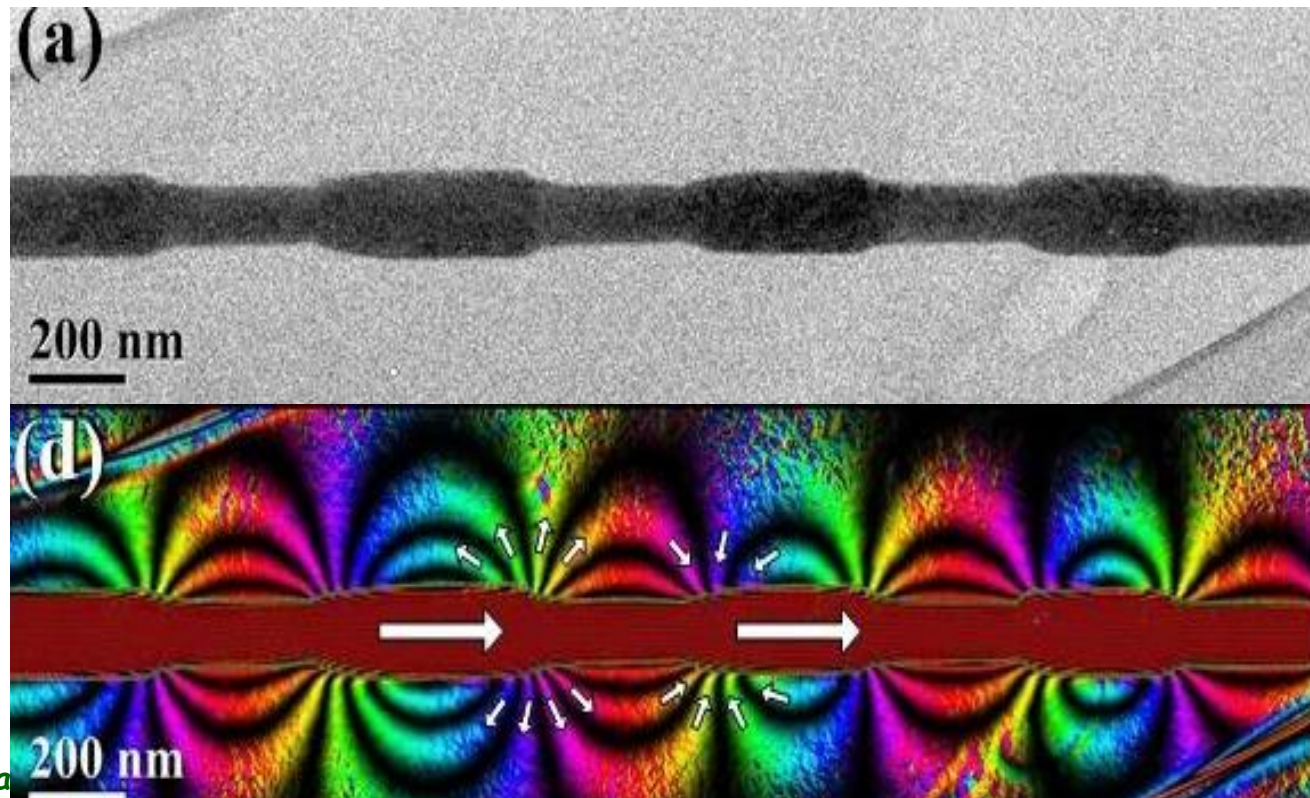


Topographic AFM (a) and Magnetic MFM (b) images of FeCo modulated NW

Interpretation of bright and dark MFM contrasts



Axial Domain and stray fields at modulations

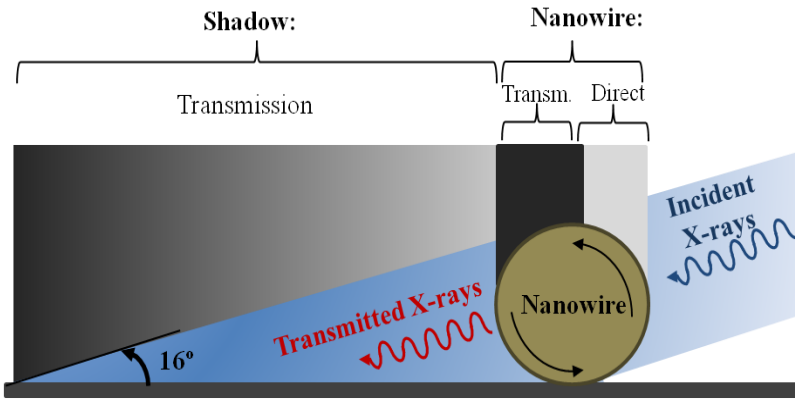


SEM (a) and Electron Holography (d) images of the magnetic flux

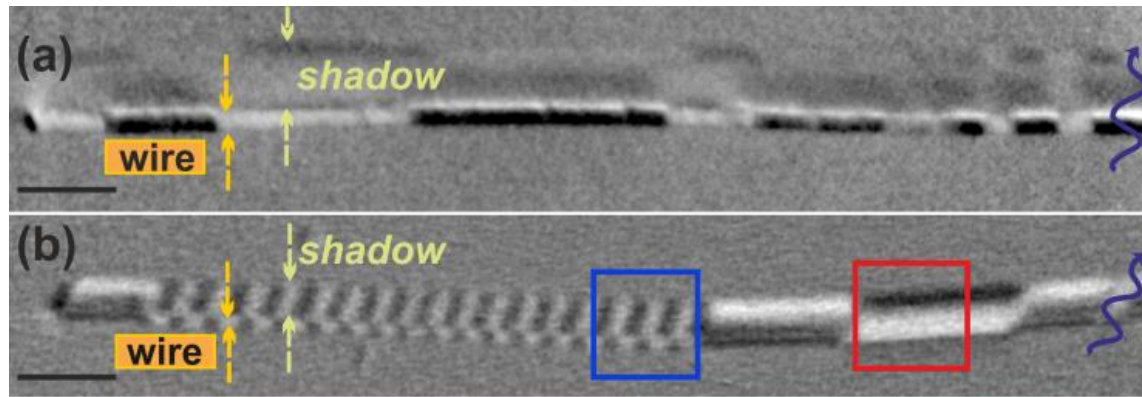
E. Snoek, Toulouse
A. Asenjo

L. Robriguez, C. Bran, E. Berganza
et al. ACS Nano 10 (2017) 9669

Photo-emission electron microscopy with X-ray magnetic circular dichroism (PEEM-XMCD): surface and bulk spin configuration

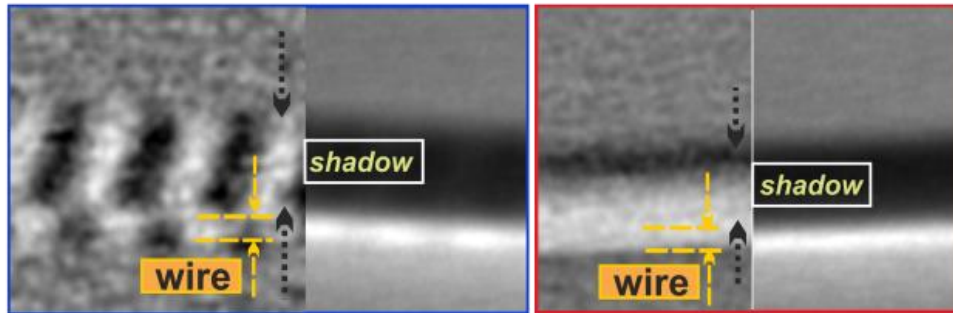


Imaging Transverse and Vortex domains



← hcp $Co_{85}Ni_{15}$

← hcp, fcc
 $Co_{65}Ni_{35}$



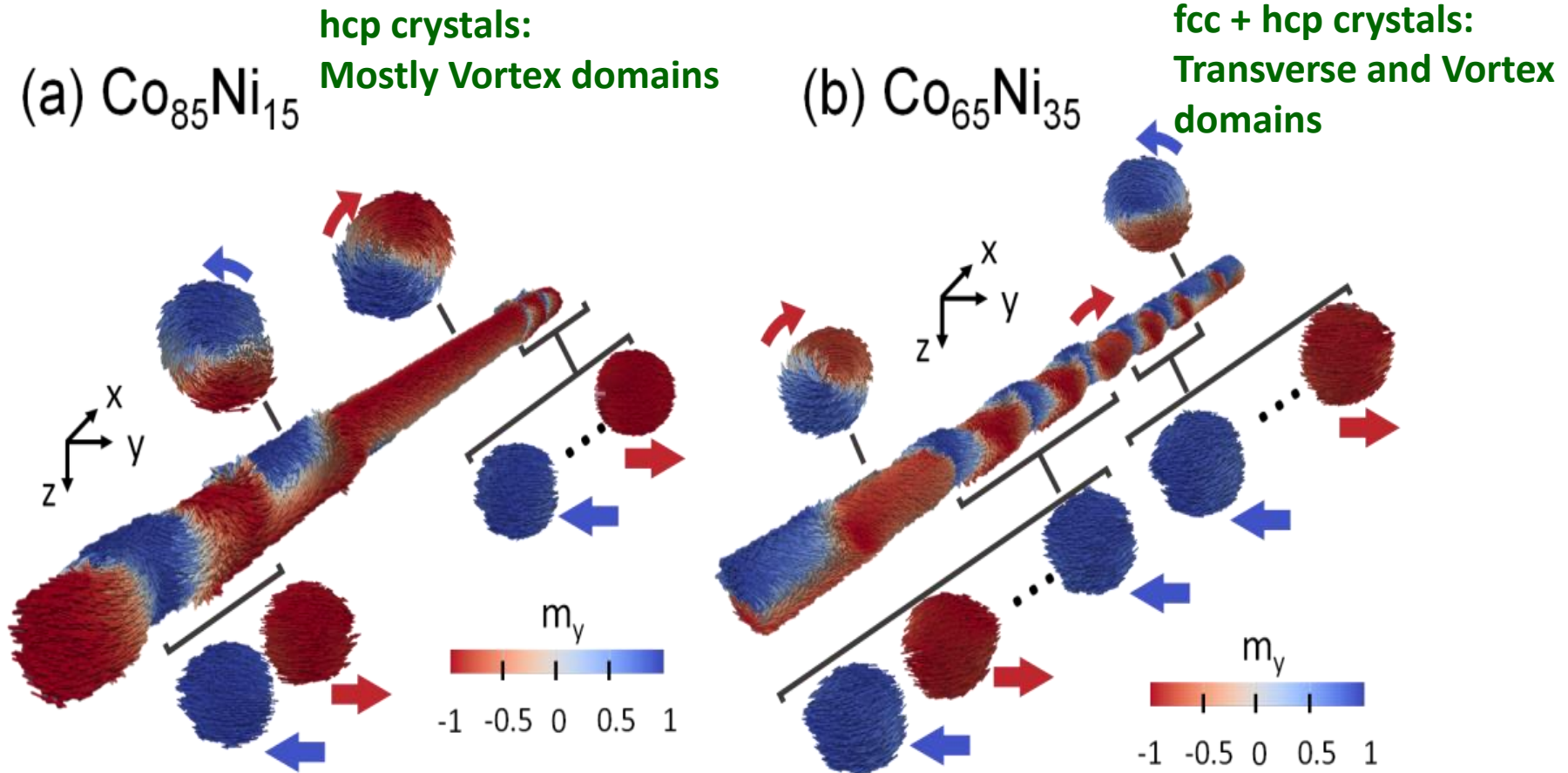
Transverse Domain

Vortex Domain

C. Bran , L. Aballe et al.
J. Mater. Chem. C 4 (2016) 978

Bran et al
(Phys Rev Sept2017)

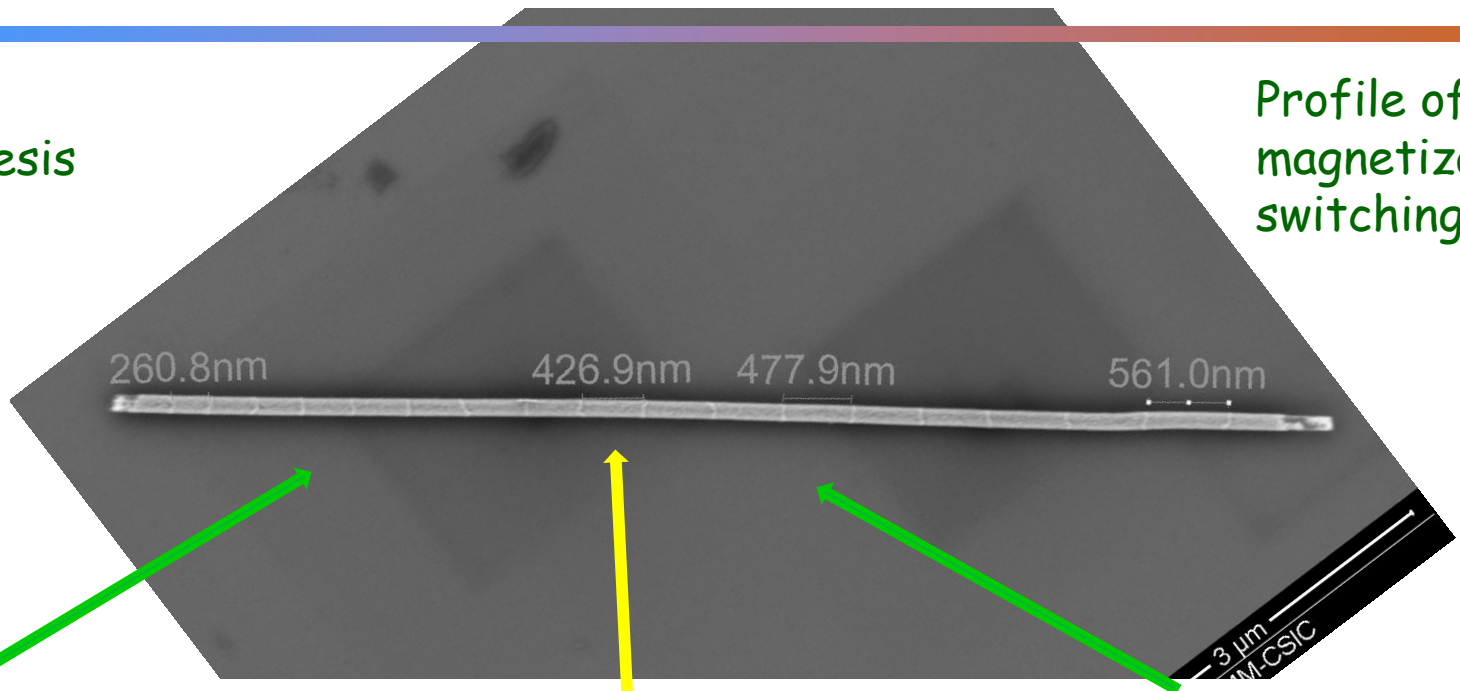
Simulated Domain Structure in CoNi alloy nanowires: Vortex and Transverse Domains



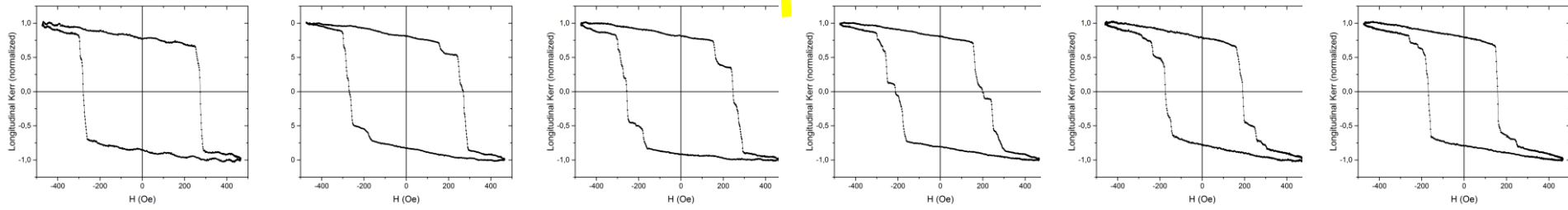
Multisegmented FeCo/Cu NWs: magneto-optic Kerr effect

Local hysteresis loops

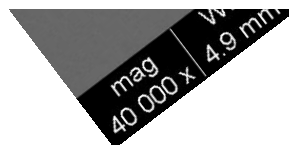
Profile of magnetization switching



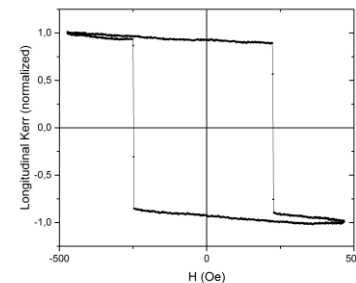
Jessi Meyer
Ester Palmero



Stepped propagation of a domain wall

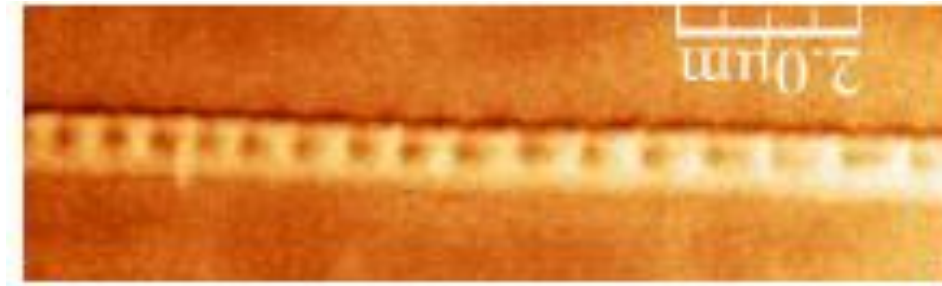


Loop of a uniform wire



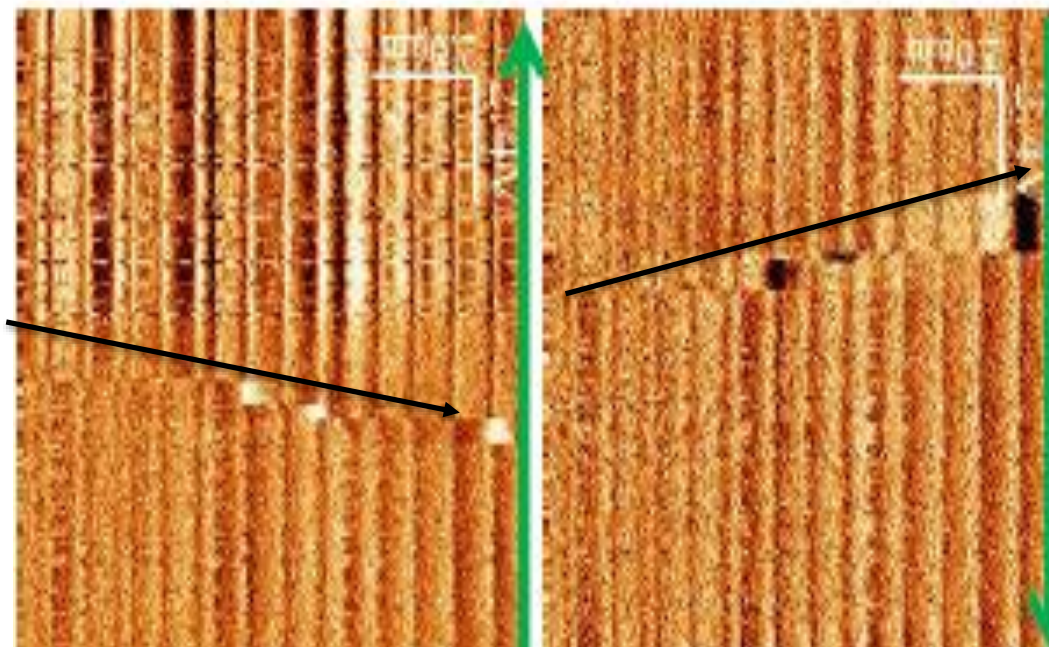
Multisegmented Nanowires, MFM imaging

FeCo/Cu with increasing FeCo segment length from one end



Eider Berganza

Unidirectional
Reversal from
short to longer
segments in
quantified steps

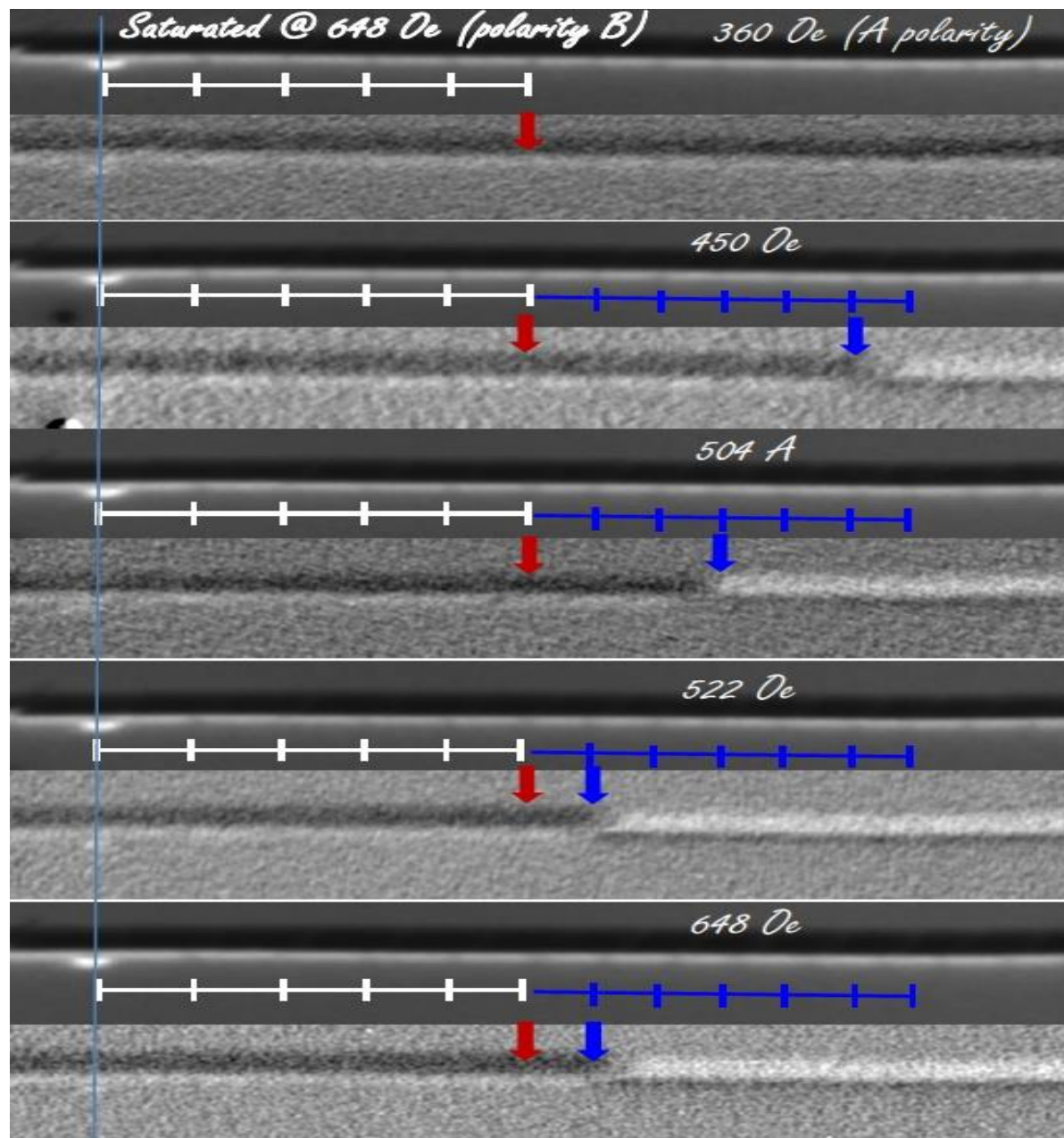


H
applied

FeCo/Cu with increasing FeCo segment length from one end

Stepped motion of the single domain wall

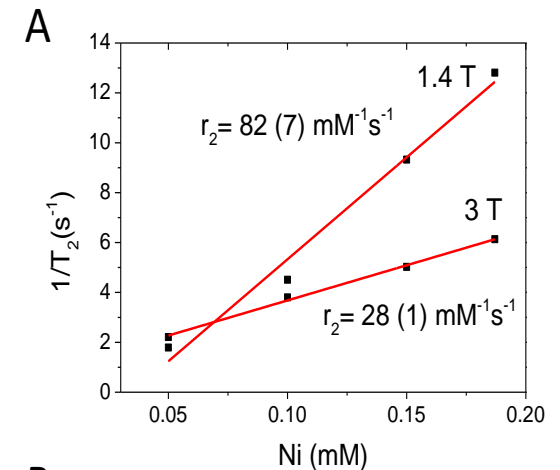
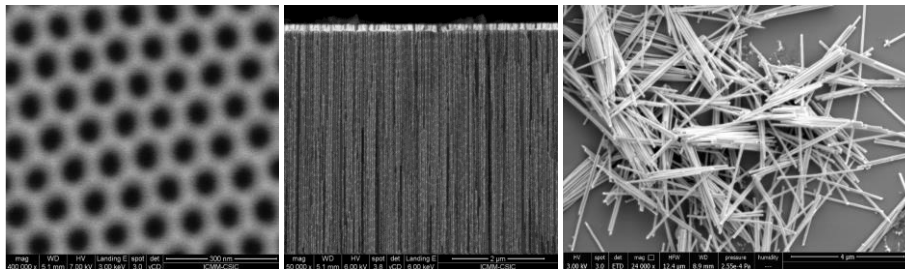
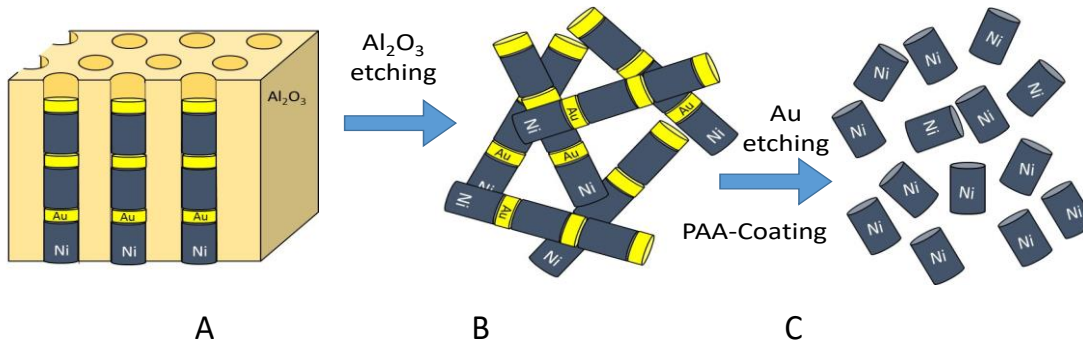
(PEEM-XMCD)



Cristina Bran

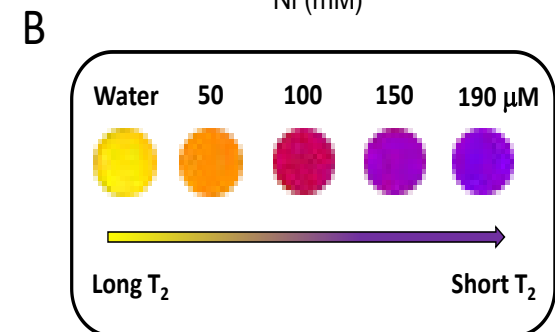
A colloiddally stable water dispersion of Ni nanopillars as efficient T_2 -MRI contrast agent

Bañobre, Rivas et al., *J.Mater.Chem. B*, 5 (2017)3283



A) Transversal relaxivity (r_2) of a water solution of PAA-coated Ni nanowires at 1.41 T and 3 T at 37 °C.

B) T_2 map of PAA-coated Ni nanowires acquired at 3 T and 37 °C.



Contactos Hispanoamericanos Latin-American Workshops



my Taiwanese Magnetic Family

Spanish Moais



Ural Federal University
named after the first President of Russia B.N.Yeltsin

LABORATORY OF MAGNETIC SENSORS

The aim of the Laboratory of Magnetic Sensors is to become a world-class center for the development of new magnetic materials and effective functional transducers on their basis.

Under the supervision of Professor Vazquez, research is being conducted (among others), on the following topics:

- Development of physical and chemical basis of synthesis technologies of new composite and film materials for sensor technologies.
- Magnetodynamics of nanostructured materials with high magnetic permeability: giant magnetoresistance, ferromagnetic resonance, non-resonant magnetosubstrations.
- Functional polymer/magnetic nanoparticles composites (in collaboration with the Institute of Electrodynamics of the Ural Branch of the Russian Academy of Sciences).
- Magnetic nanoparticles for biological applications and magnetic bioimaging.
- Film structure with exchange bias.
- Amorphous alumina membranes with ordered pores.

The Laboratory is well equipped, including specific sample preparation equipment and different magnetometry characterization techniques. A big effort is being made to renovate some of the experimental facilities, including a new fast effect magnetometer or microwave techniques.

Some of the research results obtained in the Laboratory have already been published in journals from the field of Chemistry and Physics of Materials.

International Head

Dr. Manuel Vazquez Villabarta
Professor of Research at the Institute of Materials Science of Madrid from the Spanish National Council for Research

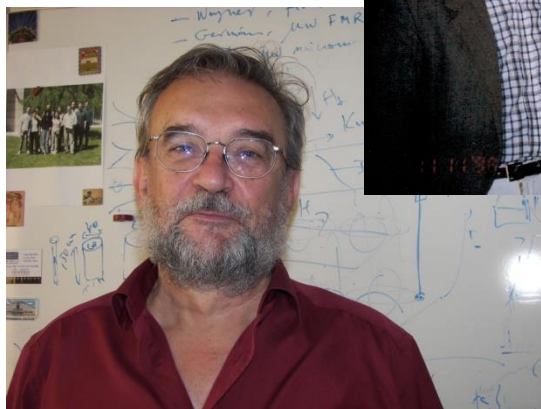
URFU Co-Head

Dr. Yaroslavsky
Department of Magnetism in Nanomaterials
Natural Sciences
yavovskiy@urfu.ru



our Siberian Magnetic Sensors Lab.

Prof. to Univ. Wuhan, China



Recientes actividades de internacionalización

IUPAP, ICM 2015



IEEE Magnetics Society Summer School Santander, 2017



INTERMAG 2017, Dublin



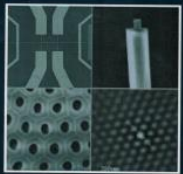
Grupo magnético: 20 doctores 30-40 postdocs y visitantes



20/12/2007 14:10



WOODHEAD PUBLISHING SERIES IN ELECTRONIC AND OPTICAL MATERIALS



Magnetic Nano- and Microwires

Design, Synthesis, Properties and Applications

Edited by Manuel Vázquez



What is the IEEE Magnetics Society ?

- a) One of 46 Societies/Councils from the IEEE (Institute of Electrical and Electronic Engineers)
- b) *MagSoc is the 52 Years old, worldwide largest (over 3,000 members) non-profit Association dealing with magnetics*
- c) *Managed by Volunteers, supported by professional administration*

Presidency of IEEE Magnetics Society, 2017-18



Constitution + Bylaws Governed by the Administrative Committee

Officers (2 years term)

President

Vice-Pres

Secretary

Past-President

24 Elected AdCom Members

+ 11 Committee Chairs

Conferences (Intermag, MMM)

Technical

Honors & Awards

Distinguished Lecturers

Education (Summer School)

Membership

Publicity

Finance

Chapters

Nominations

Publications (IEEE Trans Magn, Magn. Letters)

Join the Magnetics Society:

if interested, contact: Manuel Vazquez, at manuel.v.vazquez@ieee.org